Enclosure 2
KP-FHR Core Design and Analysis Methodology Topical Report
(Non-Proprietary)

KP-TR-024-NP

Kairos Power LLC

707 W. Tower Ave
Alameda, CA 94501

KP-FHR Core Design and Analysis Methodology

Topical Report

Revision No. 0
Document Date: April 2024

Non-Proprietary

Rev	Description of Change	Date
0	Initial Issuance	April 2024

Executive Summary

Kairos Power is pursuing the design, licensing, and deployment of a Fluoride Salt-Cooled, High Temperature (KP-FHR) reactor. To enable these objectives, the development of a technology-specific core design and analysis methodology is required. This report describes the methodology for core physics, thermal hydraulic analysis, and radiation effects on materials of the KP-FHR.

The core design methodology described within this report applies to the steady-state operation of a KP-FHR. This methodology is informed by research publications pertaining to FHRs and other pebble bed reactors. The methods are also informed by key neutronics and thermal hydraulic steady state phenomena in the KP-FHR.

The KP-FHR core design methodology is composed of the Serpent 2 nuclear design and STAR-CCM+ thermal, fluid, and discrete element modeling design codes. These codes are connected by a series of Kairos Power developed wrapper codes. The verification and validation (V&V) methodology for Serpent 2 and STAR-CCM+ codes is also described herein.

Serpent 2 and STAR-CCM+ and the associated wrapper codes are used to calculate core composition during various phases of operation and to calculate corresponding parameters such as core reactivity coefficients, control and shutdown element worth, shutdown margin, power distribution, radiation damage within and including reactor vessel, core and reflector temperature distributions. The methodology for using the codes to perform these calculations and the limitations on the use of this methodology are provided.

Additionally, this topical report presents a structured approach for quantifying uncertainty, using known uncertainties in input parameters, and capturing biases pertinent to nuclear data. A discussion is provided on informed biases and additional discretionary conservatism (DC) for defining nuclear reliability factors (NRFs).

Sample problems are provided to illustrate the methodology for performing core design calculations and determining uncertainties.

TABLE OF CONTENTS

LIST OF TABLES

LIST OF FIGURES

NOMENCLATURE

List of Abbreviations	
ACE	a compact ENDF
AHTR	advanced high-temperature reactor
ARI	all-rods in
ARO	all-rods out
CE	continuous energy
CFD	computational fluid dynamics
CHM	carbon to heavy metal atom ratio
CRAM	Chebyshev Rational Approximation Method
CSAS	criticality safety analysis sequence
CTC	coolant temperature coefficient
CVC	coolant void coefficient
DC	discretionary conservativism
DEM	discrete elements method
DHRS	decay heat removal system
ENDF	evaluated nuclear data files
FHR	fluoride-cooled high temperature reactor
FOM	figure-of-merit
FTC	fuel temperature coefficient
HTGR	high temperature gas-cooled reactor
IET	integral effect test
IPyC	inner pyrolytic carbon layer
ITC	isothermal temperature coefficient
KERMA	kinetic energy released per unit mass
KP-FHR	Kairos Power Fluoride Salt-Cooled, High Temperature Reactor
KPACS	Kairos Power Advanced Core Simulator
KPATH	Kairos Power Advanced Thermal Hydraulics
MG	multi-group

List of Abbreviations	
MTC	moderator temperature coefficient
NRC	Nuclear Regulatory Commission
NRF	nuclear reliability factor
OPyC	outer pyrolytic carbon layer
PDC	principal design criteria
PEM	pebble extraction machine
PIRT	Phenomena Identification and Ranking Table
PSP	primary salt pump
QA	quality assurance
RCS	reactivity control system
RSS	reactivity shutdown system
RTC	reflector temperature coefficient
SARRDL	specified acceptable system radiological release limit
SET	separate effect test
SiC	silicon carbide
sKPH	simplified KP-FHR model
TH	thermal hydraulics
TRISO	tri-structural isotropic
TSL	thermal scattering law
UA	uncertainty analysis
UQ	uncertainty quantification
V&V	verification and validation

1 INTRODUCTION

Kairos Power is pursuing the design, licensing, and deployment of the Kairos Power Fluoride Salt-Cooled, High Temperature Reactor (KP-FHR) technology, including non-power test reactor and commercial power reactor designs. To support these objectives, Kairos Power has developed a core design and analysis methodology applicable to the KP-FHR design.

This topical report describes the methodology for core design and analysis of the KP-FHR design during startup, power ascension, and equilibrium conditions. The report describes the methodology used to model and analyze the nuclear and thermal-hydraulic behavior of the KP-FHR core during steady-state conditions. The core design and analysis methodology is used to calculate reactivity coefficients, rod worth, power distribution, temperature distribution, flux distribution, kinetics parameters, material depletion, radiation damage and heating. These output parameters are used for other applications including fuel performance, source term, and safety analysis. The application of these methods is illustrated in an example calculation provided for demonstration purposes.

The primary tools used to model the core include the Serpent 2 and STAR-CCM+ codes and the calculational methods associated with them, which are described in this topical report. V&V of the Serpent 2 and STAR CCM+ codes is performed through higher order methods and code-to-code benchmarks. This topical report also includes a methodology to quantify the impacts of quantifiable uncertainties and to determine bias and discretionary conservatism to inform nuclear reliability factors (NRFs). This method ensures that calculated values are reported with sufficiently conservative uncertainty values to be used as input to safety analysis for the KP-FHR. The final confirmation of criticality and other core design parameters is performed during the fuel loading process and zero power testing.

Kairos Power requests Nuclear Regulatory Commission (NRC) review and approval of this topical report for the following:

- The use of Serpent 2, STAR-CCM+ and the calculational framework to calculate the parameters and figures of merit summarized in Section 3.6.
- The calculational methodology used to determine quantifiable uncertainties described in Section 5.2.3, the biases described in Section 5.2.4 and Table 5-26, and the discretionary conservatism described in Section 5.2.5 and Table 5-27.
- The validation methodology for porous media modeling and the applicability of closure models through higher order computational fluid dynamics (CFD) models described in Section 5.3 and the bias and confidence intervals stated in Section 5.3.6 to bound temperature calculations for over/underestimation.
- The methodology presented in Section 5.4 to update nuclear reliability factors (NRFs) using operational data.

Further regulatory assessment applicable to this core design and analysis methodology is provided in this section of this topical report. Section 2 of the report provides general design features of a typical KP-FHR. These features are modeled through three domains: the motion of pebble in the core (discrete element modeling), neutronics of the core and thermal hydraulics. These modeling paradigms are described in Section 3 of this topical report. Section 4 of the report provides a summary of the codes used for modeling the KP-FHR. These codes are qualified for use in accordance with the methodology described in Section 5. Section 6 provides the application of this methodology and how figures of merit and certain outputs are used for safety analysis, nuclear design and thermal hydraulic analysis. Appendices A and B with example calculations are provided to illustrate the use of this methodology.

1.1 Design Features

1.1.1 Design Background

To facilitate NRC review and approval of this report, design features considered essential to the KP-FHR technology are provided in this section. These key features are not expected to change during the ongoing detailed design work by Kairos Power and provide the basis to support the safety review. Should fundamental changes occur to these design features or revised regulations be promulgated that affect the conclusions in this report, such changes will be reconciled and addressed in future license application submittals.

The KP-FHR is a U.S. developed Generation IV advanced reactor technology. In the last decade, U.S. national laboratories and universities have developed pre-conceptual Fluoride High-Temperature Reactor (FHR) designs with different fuel geometries, core configurations, heat transport system configurations, power cycles, and power levels. More recently, the University of California at Berkeley developed the Mark 1 pebble-bed FHR, incorporating lessons learned from the previous decade of FHR pre-conceptual designs. Kairos Power has built on the foundation laid by Department of Energy (DOE)-sponsored university Integrated Research Projects (IRPs) to develop the KP-FHR.

1.1.1 Key Design Features of the KP-FHR

The KP-FHR is a high temperature reactor with molten fluoride salt coolant operating at near-atmospheric pressure. The fuel in the KP-FHR is based on the Tri-Structural Isotropic (TRISO) high-temperature, carbonaceous-matrix coated particle fuel which was originally developed for high temperature gas-cooled reactors (HTGRs) in a pebble fuel element. Coatings on the particle fuel provide retention of fission products. The reactor coolant is a chemically stable molten fluoride salt mixture, 2 LiF: BeF_2 (Flibe) which also provides retention of fission products. A primary coolant loop circulates the reactor coolant using pumps and transfers the heat via a heat exchanger. The design includes decay heat removal for both normal conditions and postulated event conditions. Passive decay heat removal, along with natural circulation in the reactor vessel, is used to remove decay heat in response to a postulated event. The KP-FHR does not rely on electrical power to achieve and maintain safe shutdown for postulated events.

Instead of the typical light water reactor (LWR) low-leakage, pressure retaining containment structure, the KP-FHR design relies on a functional containment approach similar to the Modular High Temperature Gas-Cooled Reactor (MHTGR). The KP-FHR functional containment safety design objective is to meet 10 CFR 50.34 (10 CFR 52.79) offsite dose requirements at the plant's exclusion area boundary with margin. A functional containment is defined in Regulatory Guide (RG) 1.232, “Guidance for Developing Principal Design Criteria for Non-Light water Reactors” as a "barrier, or set of barriers taken together, that effectively limit the physical transport and release of radionuclides to the environment across a full range of normal operating conditions, anticipated operational occurrences, and accident conditions." As also stated in RG 1.232, the NRC has reviewed the functional containment concept and found it “generally acceptable,” provided that “appropriate performance requirements and criteria” are developed. The NRC staff has developed a proposed methodology for establishing functional containment performance criteria for non-LWRs, which is presented in SECY-18-0096, “Functional

Containment Performance Criteria for Non-Light-Water-Reactors." This SECY document has been approved by the Commission.

The functional containment approach for the KP-FHR is to control radionuclides primarily at their source within the coated fuel particle under normal operations and accident conditions without requiring active design features or operator actions. The KP-FHR design relies primarily on the multiple barriers within the TRISO fuel particles to ensure that the dose at the site boundary as a consequence of postulated accidents meets regulatory limits. However, in contrast to the MHTGR, the KP-FHR molten salt coolant also serves as an additional distinct barrier providing retention of fission products that escape the fuel particle and fuel pebble barriers. This additional retention barrier is a key feature of the enhanced safety and reduced source term in the KP-FHR.

1.2 Regulatory Assessment

The following section provides a brief review of regulatory requirements applicable to reactor core design and analysis for the KP-FHR.

1.2.1 10 CFR Requirements

Nuclear Regulatory Commission (NRC) regulations in 10 CFR 50.34(a)(4), 10 CFR 50.34(b)(4) and 10 CFR 52.79(a)(2) require an analysis and evaluation of the design and performance of structures, systems, and components of the facility. These regulations assess the risk to public health and safety resulting from operation of the facility and determine the margins of safety during normal operations and transient conditions during the life of the facility, and the adequacy of structures, systems, and components provided for the prevention of accidents and the mitigation of the consequences of accidents. Consistent with these requirements, the KP-FHR core design and analysis methodology described in Sections 2.2, 2.3, 3, 4, and 5 is used to analyze the fuel and core during normal operation to determine margins of safe operation of the reactor core. Calculational outputs of the methods as listed in Section 3.6 and described further in Section 6, are used to further determine the adequacy of structures, systems and components that provide for the prevention and mitigation of postulated events.

1.2.2 Principal Design Criteria for the Reactor Core

The principal design criteria that apply to KP-FHR reactors are contained in the "Principal Design Criteria for the Kairos Power Fluoride Salt-Cooled High Temperature Reactor Topical Report" (Reference 1). The core design and analysis methods are used to determine the margins of safe operation for the reactor core during normal operation to demonstrate compliance with the following principal design criteria (PDCs):

<u>PDC 10, Reactor design</u>

> *The reactor core and associated heat removal, control, and protection systems shall be designed with appropriate margin to ensure that specified acceptable system radionuclide release design limits are not exceeded during any condition of normal operation, including the effects of anticipated operational occurrences.*

Together, the modeling paradigm described in Section 3.2, the modeling tools STAR-CCM+ and Serpent 2 described in Section 4, and the validation, verification and uncertainty analyses described in Section 5 provide a methodology to support designing and modeling the reactor core and the establishment of normal operational safety margins. These safety margins established for normal operation are the basis for safety analyses used to develop and determine margins to safety during postulated events described in safety analysis reports. The methods in Section 3 and the modeling tools in Section 4 of this topical report are used to establish safety limits for normal operation by determining the reactivity feedback, shutdown margin, rod worth, power distribution, temperature distribution, flux distribution, kinetics parameters, material depletion, and helium generation in the KP-FHR core. Development of this methodology to demonstrates that reactor core safety margins are not exceeded, which satisfies, in part, PDC 10.

<u>PDC 11, Reactor inherent protection</u>

> *The reactor core and associated systems that contribute to reactivity feedback shall be designed so that, in the power operating range, the net effect of the prompt inherent nuclear feedback characteristics tends to compensate for a rapid increase in reactivity.*

The modeling paradigm described in Section 3.2, the modeling tools described in Section 4, and the validation and benchmarking analyses described in Section 5.2 provide a means of demonstrating that the net effect of prompt inherent nuclear feedback on the reactor core design compensates for rapid increases in reactivity in the KP-FHR core. Methods used to determine the reactivity feedback and kinetics parameters are described in Section 4 and the qualification of those methods is described in Section 5 via benchmarking studies. Conservative uncertainties and biases are added to calculational results, thereby providing reasonable assurance that the methodology can provide results for demonstrating compliance with PDC 11.

<u>PDC 12, Suppression of reactor power oscillations</u>

> *The reactor core; associated structures; and associated coolant, control, and protection systems shall be designed to ensure that power oscillations that can result in conditions exceeding specified acceptable system radionuclide release design limits are not possible or can be reliably and readily detected and suppressed.*

The core design tools described in Section 4 are used to show compliance with PDC 12 by demonstrating that the KP-FHR core is inherently stable and that a detection system for power-oscillations is not required in the KP-FHR design. The modeling tools are used to demonstrate that the coolant temperature and fuel temperature are not coupled in such a way that when fuel temperature changes, the coolant temperature immediately changes. This is due to the thermal properties of the coolant and the robustness of the fuel.

1.2.3 Principal Design Criteria for Other Structures, Systems and Components

Several calculational outputs of the methods provided in this topical report are used in safety analysis reports to further demonstrate the adequacy of structures, systems, and components that prevent and mitigate postulated events. The core design and analysis methodology described herein provides margins to safety during normal operation and these safety margins are used as inputs (i.e., initial conditions) for safety analyses that determine margins to safety during postulated events.

<u>PDC 16, Containment design</u>

> *A reactor functional containment, consisting of multiple barriers internal and/or external to the reactor and its cooling system, shall be provided to control the release of radioactivity to the environment and to ensure that the functional containment design conditions which are safety significant are not exceeded for as long as postulated accident conditions require.*

The KP-FHR uses TRISO fuel particles (described in Section 2.1.1) and Flibe coolant (described in Section 2.1.2), the combination of which makes up the functional containment of the design. The methodology described herein is used to design the core such that core design parameters (i.e., reactivity coefficients, shutdown margin, rod worth, kinetics parameters, material depletion, flux distribution, temperature distribution, power distribution, radiation heating and damage) have margins to safety and adequately account for core changes during normal operation due to variations in fuel and coolant. The pebble peaking factor, as an output from the core design and analysis methodology, is also used to assess fuel performance. The core design and analysis methodology therefore can be used, in part, to support a demonstration of compliance with PDC 16.

PDC 25, Protection system requirements for reactivity control malfunctions

The protection system shall be designed to ensure that specified acceptable system radionuclide release design limits are not exceeded during any postulated event, accounting for a single malfunction of the reactivity control systems.

The core design and analysis methodology is used to provide calculational output (i.e., rod worth and shutdown margin) for core and fuel limits, which supports defining operational safety limits that account for a single malfunction of the reactivity shutdown system. This methodology is used in safety analysis reports which demonstrate in part, compliance with PDC 25.

PDC 26, Reactivity control systems

A minimum of two reactivity control systems or means shall provide:

(1) A means of inserting negative reactivity at a sufficient rate and amount to assure, with appropriate margin for malfunctions, that the specified acceptable system radionuclide release design limits are not exceeded and safe shutdown is achieved and maintained during normal operation, including anticipated operational occurrences.

(2) A means which is independent and diverse from the other(s), shall be capable of controlling the rate of reactivity changes resulting from planned, normal power changes to assure that the specified acceptable system radionuclide release design limits are not exceeded.

(3) A means of inserting negative reactivity at a sufficient rate and amount to assure, with appropriate margin for malfunctions, that the capability to cool the core is maintained and a means of shutting down the reactor and maintaining, at a minimum, a safe shutdown condition following a postulated accident.

(4) A means for holding the reactor shutdown under conditions which allow for interventions such as fuel loading, inspection and repair shall be provided.

The core design and analysis methodology described herein is used to perform safety analyses which demonstrate that the KP-FHR core has sufficient negative reactivity and shutdown margin to demonstrate in part, compliance with PDC 26.

PDC 28, Reactivity limits

The reactivity control systems shall be designed with appropriate limits on the potential amount and rate of reactivity increase to ensure that the effects of postulated reactivity accidents can neither:

(1) result in damage to the safety significant elements of the reactor coolant boundary greater than limited local yielding nor

(2) sufficiently disturb the core, its support structures, or other reactor vessel internals to impair significantly the capability to cool the core.

The core design and analysis methodology is used to provide core output parameters to determine reactivity control limits. Reactivity control limits protect the fuel and other reactor systems from a hypothetical rapid change in reactivity and power. Rapid changes in power and large temperature increases could cause damage to the reactor coolant flow path and/or reactor coolant boundary and impair core cooling. The core design and analysis methodology provides a means of demonstrating the margins to operating safely during normal conditions to preclude the adverse impacts of a hypothetical rapid reactivity increase. The methodology therefore can be used to demonstrate compliance with PDC 28.

<u>PDC 31, Fracture prevention of reactor coolant boundary</u>

The safety significant elements of the reactor coolant boundary shall be designed with sufficient margin to ensure that when stressed under operating, maintenance, testing, and postulated accident conditions, (1) the boundary behaves in a nonbrittle manner and (2) the probability of rapidly propagating fracture is minimized. The design shall reflect consideration of service temperatures, service degradation of material properties, creep, fatigue, stress rupture, and other conditions of the boundary material under operating, maintenance, testing, and postulated accident conditions and the uncertainties in determining (1) material properties, (2) the effects of irradiation and coolant composition, including contaminants and reaction products, on material properties, (3) residual, steady-state, and transient stresses, and (4) size of flaws.

The core design and analysis methodology is used to demonstrate the radiation damage to stainless steel material (i.e., reactor vessel 316H and weld material) does not cause failure to the reactor coolant boundary. Displacement per atom (DPA) and helium generation calculations support this demonstration and are performed using the calculational method shown in Section 6.2.3. Therefore, the methodology can be used to evaluate the expected effects of irradiation on the reactor coolant boundary and demonstrate in part, compliance with the requirements of PDC 31.

<u>PDC 34, Residual heat removal</u>

A system to remove residual heat shall be provided. For normal operations and postulated events, the system safety function shall be to transfer fission product decay heat and other residual heat from the reactor core at a rate such that specified acceptable system radionuclide release design limits and the design conditions of safety related elements of the reactor coolant boundary are not exceeded.

Suitable redundancy in components and features and suitable interconnections, leak detection and isolation capabilities shall be provided to ensure that the system safety function can be accomplished, assuming a single failure.

The core design and analysis methodology determines the heat transfer for pebble-to-pebble and pebble-to-reflector interactions during normal operation. A predictive model can be used to determine material temperatures in the core thereby demonstrating, in part, compliance with PDC 34.

2 KP-FHR CORE DESIGN FEATURES

2.1 Reactor Core General Features

The KP-FHR core is a randomly packed pebble-bed with molten fluoride salt coolant operating at high temperature and near-atmospheric pressure. The pebble-bed core fills the space created by stacked graphite blocks, and the graphite blocks maintain a coolable geometry and act as a neutron reflector. The graphite reflector blocks and pebbles are buoyant in the molten fluoride salt coolant. Engineered channels in the reflector are used to direct coolant flow, house instrumentation, and insert control elements. The vessel encloses the core barrel and reflector blocks while maintaining the coolant flow path. Pebbles are circulated through the core to manage the core composition and control excess reactivity.

In a KP-FHR reactor core, there are geometrical design features present that are explicitly captured in the DEM and neutronic analysis, described further in Section 3.3 and 3.4 respectively. These features are shown and labeled in Figure 2-1 and are representative of the typical KP-FHR design. Figure 2-2 shows the explicit geometry modeling in Serpent 2 based on the design features of the typical KP-FHR design shown in Figure 2-1.

The highest fission power density is in the pebble bed core, which is defined as the volume from the top of the converging region to the bottom of the diverging region. Core geometrical characteristics such as the conic regions and the defueling chute are designed to balance neutronic performance, heat removal, and the radial pebble residence time profile. The function of the fueling region, located at the bottom of the reactor core, is to guide the pebbles coming from the insertion line into the reactor core. The fueling region also provides space for the pebbles to enter when displaced by the insertion of the shutdown elements. The defueling chute, located at the top of the reactor core, guides the pebbles to the extraction mechanism, and serves as a low power-density region for the short-lived fission products to decay. This in-vessel decay time reduces the decay heat for the pebble handling and storage system (PHSS) thermal management and reduces the activity of the pebbles for the count-rate requirements of the burnup measurement system.

Engineered channels in the reflector are used to direct coolant flow and house instrumentation. Engineered coolant inlet and outlet channels in the reflector blocks both above and below the core are designed to reduce pressure losses while still achieving acceptable flow distribution and flow rates through the core. The reflector block design is characterized by radial and axial gaps between blocks and at the interface with the core barrel. This geometry causes a portion of the coolant flow to bypass the core region. Additional engineered channels in the reflector are also used to reduce the temperature in the reflector.

The reactivity control system (RCS) consists of control elements that insert into engineered channels in the reflector. The reactivity shutdown system (RSS) consists of shutdown elements that directly insert into the pebble bed. The control elements are used for planned power maneuvers of the KP-FHR reactor. Only the control elements are needed to achieve short-term shutdown (i.e., not considering delayed effects from xenon). To achieve the required safe shutdown conditions, the shutdown elements are inserted (assuming the highest worth shutdown element fully withdrawn).

2.1.1 Fuel and Moderator Pebbles

The KP-FHR uses the Tri-Structural Isotropic (TRISO) carbonaceous-matrix coated fuel particle design embedded in a pebble form (Figure 2-3). The fuel kernel and the coatings on the particle fuel provide retention of fission products. TRISO particles are dispersed within the fuel pebble's fuel annulus. The fuel particles can have a range of different enrichments, from depleted uranium up to the upper limit of high assay low-enriched uranium (HALEU) (i.e., 20 wt% U235).

The KP-FHR fuel pebbles are buoyant in reactor coolant under both steady state and postulated events. There are also graphite moderator pebbles in the core to enhance the moderation (i.e., increase the carbon to heavy metal atom ratio [CHM]). In steady-state operations, the pebbles circulate through the core region slowly, and fresh fuel pebbles are inserted to replace high-burnup and/or pebbles with low-fissile content, thereby maintaining the desired excess reactivity in the reactor. The PHSS inserts pebbles at the bottom of the reactor core through the pebble insertion line (PIL). The PHSS also extracts pebbles from the top of the reactor vessel during normal operations with the pebble extraction machine (PEM). Pebbles are examined for burnup and physical damage and are either reinserted into the core or directed to storage.

2.1.2 Coolant

The reactor coolant is a single phase, chemically stable, molten, fluoride salt mixture, $2LiF:BeF_2$ (Flibe) enriched in Li-7 (Reference 11) with a high Prandtl number. The coolant acts as a functional containment and provides retention of fission products that escape from any fuel defects.

2.1.3 Reflector

The reactor core itself is formed from graphite reflector blocks that enhance neutron economy and provide the structural pathway for coolant flow through the reactor. The reflector is characterized by multiple axial coolant channels to cool the graphite reflector and small gaps between blocks that result in flow bypassing the reactor core. A primary coolant loop circulates the reactor coolant using a primary salt pump (PSP) and transfers the heat to a heat exchanger for direct rejection to the atmosphere or to a secondary power conversion system.

2.1.4 Reactivity Control and Shutdown Systems

The reactivity shutdown system (RSS) is capable of shutting down the reactor by inserting shutdown elements directly into the packed pebble bed core. Reactivity control in the KP-FHR is accomplished by the reactivity control system (RCS). The RCS inserts and withdrawals control elements outside the pebble bed into the nearby side reflector. For planned power maneuvers of the KP-FHR reactor, only the control elements are used.

2.2 Reactor Core Design

The KP-FHR core contains thousands of randomly packed buoyant pebbles that slowly ascend through the reactor core. The dynamics of the reactor core are characterized by the transition from an initial startup core to an equilibrium core over time. The fuel pebbles may contain natural or depleted uranium and fuel pebbles with enriched uranium less than 20 wt% U-235 to adjust effective enrichment and core reactivity in early startup core operations. Depending on the startup and operational schemes, the core may also contain a fraction of graphite-only moderator pebbles to maintain the desired carbon to heavy metal atom (CHM) ratio. Similar to the moderator to fuel volume ratio in light water reactors, the CHM ratio is used in the KP-FHR to define the neutron moderation conditions (i.e., over-moderated or under-moderated). Mixing different pebble types facilitates maintaining the KP-FHR core in under-moderated conditions with desired excess reactivity.

When defining the desired CHM ratio, it is also important to recognize the role of the reactor coolant. Flibe is a moderator but also an absorber due mainly to lithium-6, a natural isotope of lithium (7.59% abundance) with a large thermal absorption cross section. Enriching lithium in Li-7 is required for acceptable core performance (i.e., fuel utilization) and it also ensures negative coolant temperature reactivity feedback.

An increase in the temperature of Flibe leads to a decrease of its density with two competing reactivity feedbacks: a positive feedback due to reduced absorption and a negative feedback due to reduced moderation by the Flibe. The balance of these effects is a function of the CHM ratio (spectrum); therefore, the combined reactivity feedback can be designed to be negative by controlling the CHM ratio. After some period of operation, Li-6 is consumed, and its concentration is lower than in fresh Flibe. Li-6 in Flibe is also produced by (n,α) reactions on Be-9, leading eventually to an equilibrium concentration. Salt impurities that are present in fresh Flibe are also parasitic absorbers in addition to the accumulation of other corrosion material, each of which may have an impact on the coolant reactivity coefficients. The properties and specifications for the reactor coolant are described in Reference 11.

The ability to control the mixture of pebble types in the core allows excess reactivity to be minimized during startup and the transition core (i.e., the core representative of compositional transitions during power ascension). Core reactivity is also controlled by the movement of the control elements. Shutdown elements are also available for insertion for safe shutdown during all core states.

During normal operating conditions, thermal power generated within the fuel is transferred by conduction to the pebble surface. The thermal energy is mainly transferred via convection from the pebble surface by the coolant that flows through the randomly packed bed. At the same time, a smaller portion of the thermal energy is transferred by a mixed regime of conduction and thermal radiation, specifically, pebble-to-pebble heat conduction through a stagnant fluid, pebble-to-pebble conduction, and pebble-to-pebble radiation. A fraction of the total power is deposited in pebbles, Flibe, the reflector blocks, and surrounding structures by radiation heating.

Coolant flows through the vessel downcomer and then through the core, engineered flow channels, and a portion of it bypasses the core through gaps, channels and penetrations within the vessel internal structures. The thermal energy balance within the reactor core determines the temperature distribution within the fuel, moderator, and reflector, and for the coolant that flows through the reactor. The temperature distribution is an input for core reactivity levels, burnup calculations, and power shape.

2.3 Operational Regimes

Each period of core operation is unique in its average core composition. There are four main periods of core operation in the life of the KP-FHR reactor with respect to criticality and composition modeled in the methodology: startup (including low power), power ascension (transition core), approach to equilibrium, and equilibrium. Figure 2-4 provides an illustration of these stages. The methodology for reactor startup modeling considers both a mixed bed approach, and a critical height approach to an initial fuel load and the approach to criticality. Either approach can be supported by the methods described in this topical report.

A mixed bed approach incrementally offloads and then reloads the core with larger amounts of fissile material. At each step, subcritical multiplication measurements are performed. Each successive pebble loading is determined by the 1/M method until the core achieves criticality. For the critical height approach, the core is loaded with no fissile material. The height of the core is increased by adding fuel until criticality occurs. Predictions for each step of fuel loading is determined by the 1/M method.

At full power (or at the initial power plateau), the approach to the equilibrium core begins. At startup, the core radionuclide inventory is mostly composed of fresh fuel, and significant burnup on fresh fuel has not yet been accumulated. To compensate for burnup as it accumulates, fresh fuel pebbles are added, and depleted fuel pebbles and natural or depleted uranium pebbles (if present) are removed at a rate that maintains desired core reactivity. After some period of power operation, the isotopic concentration in the core will be largely unchanged. A stable rate of insertion and extraction of fuel will be reached, at which point, the equilibrium core has been reached.

Figure 2-1 Overview of a KP-FHR Design

[[

]]

Figure 2-2 Explicit Serpent 2 Model

[[

]]

Figure 2-3 KP-FHR Fuel Pebble and Particle Design

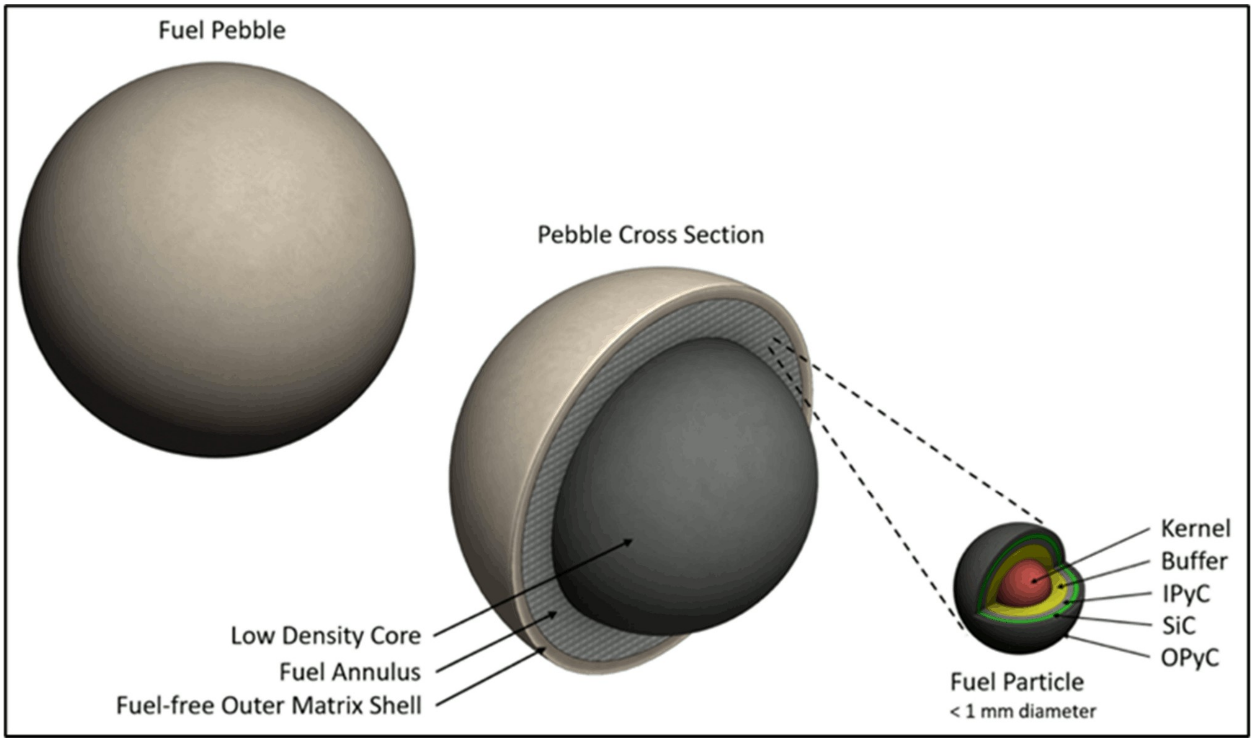

Figure 2-4 Operational Regimes of a KP-FHR

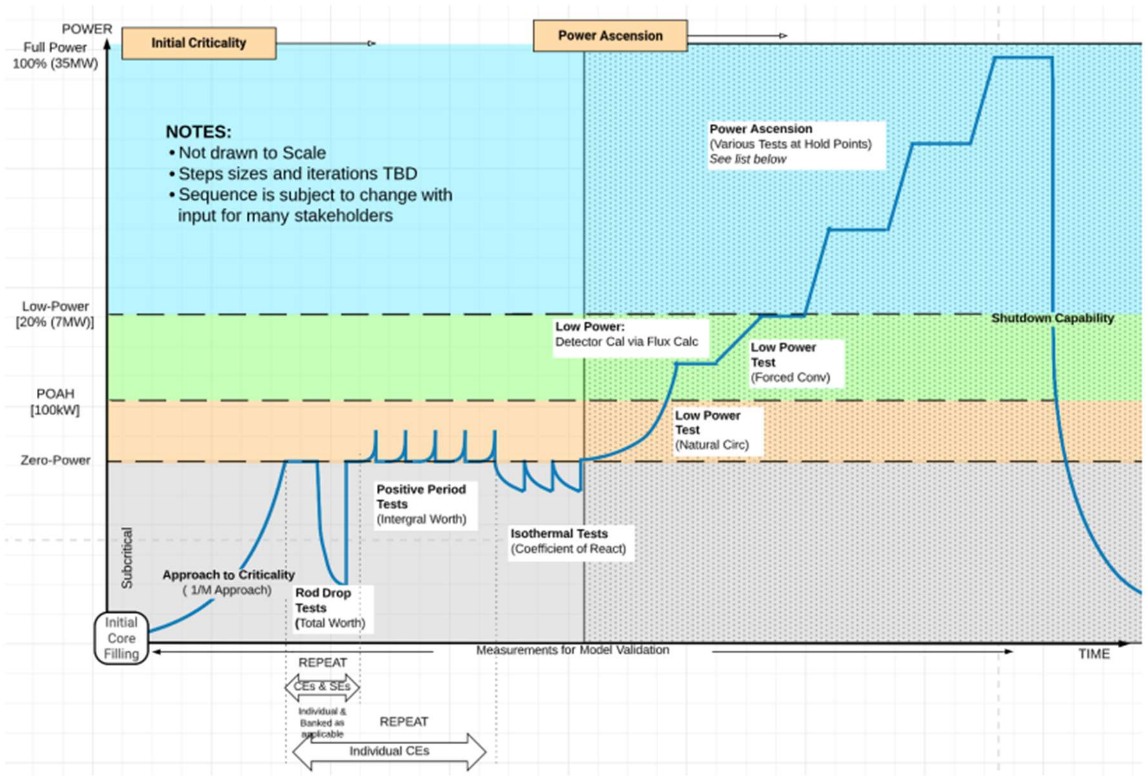

3 CORE MODELING PARADIGMS

The KP-FHR core configuration is heterogeneous and non-stationary. The pebble bed evolves from the early startup phase and approaches a statistically steady burnup equilibrium condition. KP-FHR core physical characteristics such as core geometry, heterogeneity, and pebble bed motion require unique modeling approaches. As such, the methods for modeling align very closely with the physical behavior of the core leveraging the modeling tools described in Section 4. The following sections apply to both a KP-FHR power reactor and a KP-FHR test reactor.

3.1 Key KP-FHR Core Steady-State Phenomena

Key phenomena were determined with Phenomena Identification and Ranking Tables (PIRTs), sensitivity studies, industry literature and best practices. These key phenomena and the methods used to determine their importance are discussed in the following sections.

3.1.1 Key Neutronics Phenomena

A PIRT evaluation was conducted for the KP-FHR steady-state core design. A full review of the existing Georgia Institute of Technology FHR neutronics PIRT (Reference 2), which uses the Advanced High-Temperature Reactor (AHTR) reactor design as the basis, was performed prior to beginning the KP-FHR PIRT. The description of Figures of Merit (FOMs) and knowledge level numbering used in the PIRT are as follows:

- FOM 1: Multiplication factor (1: Low impact, 2: Medium impact, and 3: High impact)
- FOM 2: Power distribution (1: Low impact, 2: Medium impact, and 3: High impact)
- Knowledge: Knowledge level (1: Low impact, 2: Medium impact, and 3: High impact)

The outcome of benchmarking the methodology against the PIRT revealed adequacy of the fidelity in the best estimate methods to capture the physics of the FHR core. A summary of the KP-FHR PIRT results is provided in Appendix C: Neutronics PIRT Results for the KP-FHR.

For phenomena with Medium or Low knowledge level and Medium to High impact, [[

]]

3.1.2 Key DEM Phenomena

Discrete elements method (DEM) accounts for the random packing and granular motion of pebbles in the core by modeling and predicting the following FOMs:

- FOM1: Static pebble center locations and packing fraction.
- FOM2: Average pebble track and velocity profiles.

The FOMs above are influenced by the following factors:

- Core shape geometry
- Pebbles contact forces
- Pebbles drag forces
- Pebbles buoyant force

DEM modeling features capture the phenomena listed above. [[

]]

3.1.3 Key Thermal Hydraulics Phenomena

The core thermal hydraulics scope is to predict steady-state temperature distributions for:

- FOM1: Core materials (Flibe, pebble, TRISO particles)
- FOM2: Reflector graphite

The phenomena for steady state conditions listed below are the same as those in the Kairos Power thermal fluid PIRT and influence the FOMs above. Phenomenon importance in the thermal fluid PIRT was determined for postulated events outside the scope of core thermal-hydraulics applications. Sensitivity analyses for nominal steady state conditions indicate that the following phenomena are of importance:

[[

]]

The following thermal-hydraulic modeling features allow capture of the phenomena listed above.
[[

]]

[[

]]

Fast neutron fluence and temperatures are used to inform geometrical and thermophysical property correlations that are then used as inputs to the thermal hydraulic model. Total core power and vessel inlet/outlet Flibe temperatures determine the system steady-state nominal flow rate.

3.2 General Modeling Approach

The KP-FHR core modeling paradigm includes discrete elements methods (DEM) (see Section 3.3), neutronics (see Section 3.4), and thermal hydraulics (TH) (see Section 3.5) modules with appropriate coupling between these domains.

DEM simulations generated by STAR-CCM+ (described further in Section 4) are used to explicitly predict the pebble distribution and velocity profile within the core and provide input to the neutronics calculations. The domain of interest for DEM is illustrated in Figure 3-1. DEM simulations use the core shape, the pebbles, and the coolant flow through the core, as input to perform calculations. The core shape, where the pebbles reside, is defined by the reflector structure, which includes the cylindrical section of the core, the upper and lower conic regions, the defueling chute, and the fuel insertion region. Therefore, the DEM modeling paradigm can use this geometry (Figure 2-1 as an example) to provide the boundaries for determining pebble distributions within the core.

The neutronics analyses of the KP-FHR core explicitly account for the double-heterogeneity of TRISO particles and pebbles. The domain of interest for the neutronics analysis is illustrated in Figure 3-1. The explicit neutronics model of the core and reflector structure in Serpent 2 informs the thermal hydraulic model power distribution, which is used to provide material temperature distribution. The neutronics model uses Serpent 2 burnup capabilities to perform depletion calculations. The neutronics model uses a full-core three-dimensional geometry (e.g., Figure 2-1), including the core and pebble bed (which accounts for pebble distributions from DEM simulations), the defueling chute, fueling region, reactivity shutdown system (RSS), reactivity control system (RCS), graphite reflector, reflector penetrations, core barrel, downcomer, and reactor vessel. Like the DEM modeling paradigm, the neutronics modeling paradigm is explicit and uses the geometry of the core.

Thermal hydraulic calculations are performed in three-dimensions using STAR-CCM+. The calculational boundaries are illustrated in Figure 3-1 and include the core, defueling chute, fueling region, and the reflector structure with full geometrical resolution (e.g., Figure 2-1), including channels, penetrations, gaps between block columns, gaps between the reflector and core barrel, gaps through vertical and horizontal reflector keys and bypass through the natural circulation flow path to account for bypass flow. The thermal hydraulic modeling of the core region is done through porous media approximation (common in pebble-bed reactor core modeling, e.g., Reference 10 and Reference 12).

[[

]]

Core analysis calculates quantities of interest for the input into safety analysis, nuclear design, fuel performance, and source term calculations. The domains of interest for modeling are determined before performing core analysis and include the geometric and material boundaries. The transfer of information used as input for applications of this methodology is managed for compliance with appropriate quality assurance requirements. The DEM, neutronics, and thermal hydraulic models are discussed further in the following sections.

3.3 DEM Modeling Paradigm

The DEM model uses a Lagrangian formulation to describe pebble equations of motion. As described in Section 3.2, STAR-CCM+ is used for both DEM and thermal hydraulic modeling. DEM simulations are performed with a separate module of STAR-CCM+ that uses the pebble geometry, pebble mechanical properties, reflector CAD model (described in Section 2.1.3), reflector mechanical properties, Flibe thermophysical properties, [[ ]]

DEM Lagrangian formulation uses momentum conservation equations for each pebble, and considers buoyant, drag, and contact forces as shown in Equation 1 below where $m_p$is the pebble mass and $v_p$is the pebble velocity:

$$m_p \frac{dv_p}{dt} = \vec{F}_{Drag} + \vec{F}_{Buoyant} + \vec{F}_{Contact} \quad (1)$$

The Flibe flow across the core creates drag forces on pebbles in the packed bed. The influence of fluid drag on pebbles flow is unique to the KP-FHR design in which pebbles are positively buoyant. [[

]]

[[

]] This collected DEM data provides a statistical basis for neutronics and thermal hydraulic calculations to derive the following FOMs:

- FOM 1: Static pebble center locations and packing fraction
- FOM 2: Average pebble tracks and velocity profiles

The above FOMs are used as inputs for neutronics and thermal hydraulic applications. The pebble center locations are used to generate randomly packed pebble bed geometries for neutronics calculations and to provide global packing fraction (porosity) for the thermal hydraulic porous model.

DEM provides detailed information for the transient pebble trajectories inside the core and their statistical average provides input for burnup calculations performed using KPACS (described in Section 4.4.3). The methodology to calculate average pebble trajectories and velocity considers the recirculation of the pebble from core inlet to extraction point at the core outlet. The ZONER tool, described in Section 4.4.3.1, post-processes the DEM simulation outputs to generate spectral zones in the core.

The major model inputs to DEM are:

- Core and pebbles geometry
- Operating conditions (i.e., flow rate)
- Pebble mechanical properties
- Reflector mechanical properties
- Flibe thermophysical properties
- Tribology data for coefficient of friction (COF)

3.4 Neutronics Modeling Paradigm

Explicit neutronics modeling of the KP-FHR core design features (see Section 2) is performed using Serpent 2, which is described further in Section 4.3. Serpent 2 is a continuous-energy Monte Carlo (MC) radiation transport code that provides high-fidelity calculations.

The model is composed of explicitly modeled pebbles in the core, each with a defined pebble type and composition. TRISO particles are also explicitly modeled within the pebble. As summarized in Section 3.2, the Serpent 2 model includes the graphite reflector with major engineered penetrations and Flibe flow path geometries within the reflector explicitly modeled (see Figure 2-2 based on typical KP-FHR geometry). The reflector region is modeled as a material that homogenizes the Flibe volume fraction and the bulk graphite block. This homogenization accounts for Flibe in the coolant channels (converging and diverging region), gaps between blocks, upper expansion wells, and other minor features. Sections of the reflector with different Flibe fractions can be modeled separately based on the model fidelity required. The neutronic modeling of Flibe regions in the reflector as homogenized material is appropriate because of the small geometric dimensions relative to the neutron mean free path, relatively small Flibe quantity, and the smearing effect of azimuthal symmetry. The modeling of the RSS and RCS elements include the neutron absorber material and cladding and conservatively neglect the neutronic impact of other structural material.

The reactor is modeled neutronically within the boundaries described in Section 3.2 (i.e., Figure 3-1), and is used to model various core states or material compositions. Material compositions are defined using available specifications, best-available estimates, and conservative estimates. Impacts on material composition uncertainty are considered and quantified in Section 5.2.3. Temperature feedback effects in the reactor are analyzed using KPATH, described in Section 4.4.4.

The nuclear data files used by Serpent 2 are produced by NJOY21 with inputs defined by KACEGEN, which is described further in Section 4.4.2. The outputs from neutronics modeling are summarized in Section 3.6. The calculational methodologies for deriving the FOMs are described in Section 6.1. The KP-FHR reactor is modeled with the general features described in Section 2 and due to the reactor design, the Serpent 2 model can be modified or expanded as necessary to represent different neutronics phenomena and calculate the figures of merit (FOMs) in Section 3.6.

3.5 Thermal Hydraulics Modeling Paradigm

Table 3-1 provides an example of general thermal hydraulic parameters of KP-FHR test reactors during normal steady state operations. The FOMs for the thermal hydraulic analyses of the KP-FHR are:

1) Core materials temperature distribution
2) The graphite reflector temperature distribution

Thermal hydraulic analyses are used to update material cross section temperatures for reactivity calculations and to provide fuel and reflector temperature distributions (with associated uncertainties) to ensure operation within steady-state qualification limits.

Core thermal hydraulics modeling is applicable to steady-state KP-FHR core operations, assuming the modeled conditions are within the range of applicability in the constitutive models. [[

]]

A local thermal non-equilibrium (LTNE) porous media (PM) model (References 10, 12, and 17) is used to model the packed bed core mass, momentum, and energy transport. The model provides a macroscopic volume averaged representation of pebbles to determine fluid flow and heat transfer. To close mathematical model formulations, the methodology uses correlations for pressure drop and heat transfer.

[[

]]

The neutronics model provides power density fields for core and reflector regions as an input to the thermal-hydraulics model. The FHR power shape is not sensitive to temperature feedback, therefore a one-way coupling is used as the baseline modality of data transfer for thermal hydraulics (Reference 18). A two-way coupling calculation using the KPATH tool is described in Section 4.4.4 and has been performed to validate this assumption.

3.5.1 Porous Media Model

This section describes the three correlations that are used for packed bed porous media momentum and heat transfer modeling. The applicability of correlations is assessed for a range of operations where the methodology applies, as described in Section 5.3. Table 3-3 provides a summary of the non-dimensional numbers used in these correlations and their definitions.

3.5.1.1 Pressure Drop Correlation

The KTA correlation (Reference 7) is used to model the pressure drop across the packed bed as expressed in Equations 5 and 6:

$$\frac{\Delta P}{\Delta H} = \Psi \frac{1-\epsilon}{\epsilon^3} \frac{1}{D_p} \frac{1}{2\rho} \left(\frac{\dot{m}}{A}\right)^2 \tag{5}$$

$$\Psi = \frac{320}{\left(\frac{Re_p}{1-\epsilon}\right)} + \frac{6}{\left(\frac{Re_p}{1-\epsilon}\right)^{0.1}} \tag{6}$$

where $\Delta H$is the height of the bed and ϵ is the porosity of the bed. KTA correlation implementation in the porous media model is discussed further in Section 3.5.1.3.

3.5.1.2 Heat Transfer Correlation

The Wakao correlation (Reference 8) as shown in Equation 7, is used to model the fluid-to-pebble heat transfer in the packed bed:

$$Nu_w = 2 + 1.1\, Pr^{1/3}\, \mathrm{Re}^{0.6} \tag{7}$$

[[

]]

Section 4.3.1.3 describes how these correlations are implemented in the porous media model formulation.

3.5.1.3 LTNE Porous Media Formulation

The local thermal non-equilibrium (LTNE) porous media formulation is used for the core region only. LTNE is used to capture the convective heat transfer between pebbles and Flibe. In this formulation, the pebbles and Flibe have different temperatures. Flibe is referred to as "fluid-phase" and pebbles referred to as "solid-phases." The LTNE formulation for mass, momentum, and energy transport for Flibe and pebbles (i.e., fuel pebbles and graphite pebbles) are presented below. The implementation of pressure drop and heat transfer correlations are also provided below. Examples of applications of LTNE are found in References 10 and 12. The LTNE porous media model also models power distribution between core materials as shown in Table 3.5. The LTNE porous media model provides the surface average temperature of pebbles. To model the temperatures within the pebbles and TRISO particles, a 1D thermal conduction model is implemented and uses the pebble surface temperature from porous media as a boundary condition as shown in Figure 3-3.

The geometrical characterization of the packed bed is described by three inputs. Porosity ϵ, represented in Equation 9, solid-phase volume fraction α_{si}, represented in Equation 10, and interaction area density a_{wi}, represented in Equation 11. The latter represents the i-th solid-phase surface area per unit volume inside the bed.

$$\epsilon = \frac{V_{fluid}}{\mathrm{V}_{bed}} \tag{9}$$

$$\alpha_{\mathrm{si}} = \frac{V_{solid,i}}{\sum_i V_{solid,i}} \tag{10}$$

$$a_{\mathrm{wi}} = \alpha_{\mathrm{si}} \frac{6(1-\epsilon)}{D_p} \tag{11}$$

Where, $V_{solid,i}$ is the volume of the i-th solid porous phase (e.g., fuel pebbles and graphite pebbles), ϵ is the core porosity and D_p is the pebble diameter.

An example of derivation for the LTNE formulation can be found in Reference 12, and it is based on the application of a volume average operator to the mass, momentum, and energy equations for fluid and solid porous media phases.

The steady-state formulation includes the following transport equations:

- Flibe mass conservation
- Flibe momentum transport
- Flibe energy transport
- Pebbles energy transport

The transport equations are based on the physical velocity formulation that accounts for the increase of fluid velocity when it enters the porous medium. The relation between physical velocity and superficial velocity (the Dupuit-Forchheimer relation in Reference 17) is shown in Equation 12:

$$\overrightarrow{v_s} = \epsilon\,\vec{v} \tag{12}$$

Where $v_s$is the superficial velocity, $v$is the physical velocity and ϵ is the porosity.

Flibe Mass Conservation Equation

The Flibe-phase mass conservation equation is represented by Equation 13, where $\rho_f$is the Flibe density:

$$\nabla\left(\epsilon \rho_f \vec{v}\right) = 0 \tag{13}$$

Flibe Momentum Transport Equation and KTA Correlation Implementation

Flibe-phase momentum transport is represented by Equations 14, 15 and 16:

$$\nabla\left(\epsilon \rho_f \vec{v}\vec{v}\right) = -\epsilon \nabla P + \nabla(\epsilon \boldsymbol{T}) - \epsilon\overrightarrow{f_p} + \epsilon\overrightarrow{f_b} \tag{14}$$

$$\boldsymbol{T} = \mu_f(\nabla\vec{v} \;+\; \nabla\vec{v}^T) - \frac{2}{3}\mu_f(\nabla\cdot\vec{v}\,)\boldsymbol{I} \tag{15}$$

$$\overrightarrow{f_b} = \rho \vec{g} \tag{16}$$

where, P is the pressure, *T* is the velocity shear stress tensor, *I* is the Identity tensor, f_p is the porous resistance force, f_b is the body force and μ_f is the fluid viscosity.

The porous resistance force, shown in Equation 17, is expressed in the form of Dupuit-Darcy-Forchheimer (References 12, 17, 19, and 20) to account for linear and quadratic superficial velocity components of pressure losses typical of porous media (Reference 17):

$$\overrightarrow{f_p} = P_v \overrightarrow{v_S} + P_i |\overrightarrow{v_s}| \overrightarrow{v_s} \tag{17}$$

where P_v is the viscous porous isotropic resistance tensor and P_i is the inertial porous isotropic resistance tensor.

The KTA correlation is implemented by re-arranging its original formulation (Reference 7) in Dupuit-Darcy-Forchheimer form as isotropic resistance tensors, Equations 18 and 19:

$$\boldsymbol{P_v} = 160 \frac{(1-\epsilon)^2 \mu}{\epsilon^3 D_p^2} \tag{18}$$

$$P_i = 3 \frac{(1-\epsilon)\rho_f}{\epsilon^3 D_p} \left(\frac{Re_p}{1-\epsilon}\right)^{-0.1} \tag{20}$$

The KTA porous resistance force can be implemented as described in Equation 21:

$$\overrightarrow{f_p} = 160 \frac{(1-\epsilon)^2 \mu}{\epsilon^3 d_p^2} \vec{v}_s + 3 \frac{(1-\epsilon)\rho_f}{\epsilon^3 d_p} \left(\frac{Re_p}{1-\epsilon}\right)^{-0.1} \vec{v}_s |\vec{v}_s| = \nabla P_d \tag{21}$$

In Equation 21, ρ_f is the density of Flibe, $\vec{v}_s$ is the Flibe superficial velocity vector, ϵ is the average bed porosity, d_p is the pebble diameter, μ is the Flibe viscosity, and Re_p is the Reynolds number based on pebble diameter and superficial velocity. Equation 21 also models the pressure gradient vector ∇P_d used in DEM models to model pebble drag force. The pressure gradient is extracted and implemented as pebble volumetric body force. This has been described in Section 3.5.

Flibe Energy Transport Equation and Wakao Correlation Implementation

The Flibe-phase energy transport equation is represented in Equation 22:

$$\nabla\left(\epsilon \rho_f H_f \vec{v}\right) = -\nabla\left(\epsilon \overrightarrow{q_f''}\right) + \nabla(\epsilon \boldsymbol{T} \vec{v}) + \sum_{\substack{solid \\ phases}} a_{\mathrm{wi}}\, HTC_{si} \left(T_f - T_{si}\right) + \epsilon \overrightarrow{f_b} \cdot \vec{v} + S_f^e \tag{22}$$

where the heat flux is defined as:

$$\overrightarrow{q_f^{"}} = -k_f \nabla \mathrm{T_f} \tag{23}$$

And where H_f is the total enthalpy of the fluid, k_f is the fluid thermal conductivity, HTC_{si} is the heat transfer coefficient for the fluid-solid phase for the i-th solid phase, S_f^e is the volumetric energy source term (power deposited in Flibe), T_f is the local mass flow averaged temperature of the fluid, and T_{si} is the local average surface temperature of the i-th solid phase.

The Wakao correlation (References 8 and 21) is implemented by expressing the energy equation in terms of heat transfer coefficient as shown in Equation 24:

$$\mathrm{HTC_{si}} = Nu_w \frac{k_f}{D_p} = \frac{k_f}{D_p}\left(2 + 1.1\, Pr^{1/3}\, \mathrm{Re}_p^{0.6}\right) \tag{24}$$

The correlation is used to express heat transfer between the Flibe and pebbles (i.e., fuel pebbles and moderator pebbles).

Pebbles Energy Transport Equation

The pebble-phase energy transport equation is provided in Equation 25:

$$-\nabla\left[(1-\epsilon)\alpha_{\mathrm{si}}\overrightarrow{q"_{si}}\right] + a_{\mathrm{wi}}\ \mathrm{HTC_{si}}\left(T_{si} - T_f\right) + S_{si}^e = 0 \tag{25}$$

where the heat flux is defined as:

$$\overrightarrow{q_{si}^{"}} = -k_{si,eff} \nabla \mathrm{T}_{si} \tag{26}$$

And where $k_{si,eff}$ is the i-th effective solid thermal conductivity and S_{si}^e is the volumetric energy source term for i-th solid phase (power deposition in the i-th solid phase)

The effective solid thermal conductivity refers to the fuel pebbles layers thermal homogenization. Two equations of this form are used, one for fuel-pebbles and one for graphite pebbles. The model does not account for fuel-to-moderator pebble heat transfer due to negligible radiation and contact heat transfer.

Core-Reflector Boundary Conditions [[ ]]

[[

]]

[[

]]

Pebble and TRISO 1-D Heat Transfer Model

Power is expressed in the form of power density distributions from the coupled neutronics model and is defined in the equations as volumetric source term in the corresponding porous-phase energy formulation.

The LTNE model provides the fuel pebble outer surface temperature distributions. The fuel pebble surface temperature field is used as a boundary condition for the 1D pebble model. The one-dimensional TRISO model is connected to a reference temperature within the pebble fuel layer.

Pebble power, $\dot{Q}_{PB}$, shown in Equation 30, is evaluated from the power density pebble peaking factor distribution shown in Equation 31:

[[

]]

[[

]]

The TRISO one-dimensional model uses a reference temperature of the pebble fuel layer as an outer boundary condition as shown in Figure 3-4. TRISO power shown in Equation 34 is evaluated from the corresponding pebble power and a constant TRISO peaking factor. The fuel kernel is the only region modeled with a power source. PF_{TRISO} in Equation 34 represents the TRISO power peaking within the pebble fuel layer. [[

]]

[[

]]

3.5.2 Reflector Modeling

[[

]]

3.5.3 Thermal Hydraulic Model Use

The core thermal-hydraulics methodology uses [[

]]

[[

]]

[[

]]

3.6 Summary of Calculational Outputs

Using the modeling paradigms and boundaries described above for core analysis, the following calculated output quantities for different core states are determined and used in core design as noted below:

[[

]]

The following output parameters from the core design and analysis methodology is used as input into safety analysis calculations:

- Reactivity coefficients
- Kinetics parameters
- Shutdown margin
- Rod worth
- Axial and radial power shape
- Pebble peaking factor (fuel performance)

Conservative uncertainties are applied to these parameters per the methodology provided in Section 5. Further discussion of the application of these output parameters is provided in Section 6.

Table 3-1 Example of Thermal Hydraulic Parameters of KP-FHR Test Reactors

TH Features	Hermes	Hermes 2.0
Thermal Power [MW]	[[ ]]	35
Vessel inlet/outlet temperatures [°C]	550-650	550-650
Pebble Power [W]	[[ ]]	[[ ]]
Peak TRISO SiC temperatures [°C]	770	850
Peak TRISO kernel temperatures [°C]	820	1000
Reflector peak temperatures [°C]	[[ ]]	[[ ]]
Flibe Pr	[[ ]]	[[ ]]
Core Re_P[1]	[[ ]]	[[ ]]
Core inlet/outlet channels Re_{Dh}[2]	[[ ]]	[[ ]]
Reflector cooling channels Re_{Dh}[2]	[[ ]]	[[ ]]
Reflector blocks gaps Re_{Dh}[2]	[[ ]]	[[ ]]
Core porosity	40-42%	40-42%

Notes

1. Re_P is the Reynolds number based on pebble diameter and superficial velocity.
2. Re_{Dh} is the Reynolds number based on hydraulic diameter and average velocity.

Table 3-2 Model Paradigm Summary

[[

]]

Table 3-3 Non-dimensional Numbers Definition

Number	Definition	Variables	Nomenclature
Reynolds	$Re = \frac{\rho v_s D_p}{\mu} = \frac{\dot{m} D_p}{\mu A}$	ρ	Density (kg/m^3)
		v_s	Superficial velocity (m/s)
		D_p	Pebble diameter (m)
		μ	Dynamic viscosity (Pa-s)
		A	Flow area (m^2)
		$\dot{m}$	Mass flow rate (kg/s)
Prandtl	$Pr = \frac{\mu \, C_p}{k}$	C_p	Specific heat capacity (kJ/kg K)
		k	Thermal conductivity (W/m K)
Nusselt	$Nu = \frac{HTC \, D_p}{k}$	HTC	Heat transfer coefficient (W/m^2 K)
Richardson	$Ri = \frac{g \beta \Delta T D_p}{v_s^2}$	g	Gravity acceleration (m/s^2)
		β	Thermal expansion coefficient (1/K)
		ΔT	Reference temperature difference (K)

Table 3-4 LTNE Boundary Conditions for the Core and Reflector

[[

]]

Table 3-5 Power Distributions FOM

Region	Power	Description
IN Core	Fuel	Power deposited in fuel pebbles
	Fuel Pass X	Power deposited in fuel pebbles of a given Pass X
	Graphite	Power deposited in graphite pebbles
	Flibe	Power deposited in Flibe
EX Core	Graphite	Power deposited in reflector
	Flibe	Power deposited in Flibe
	Steel	Power deposited in steel structures

Figure 3-1 Core Modeling Domains

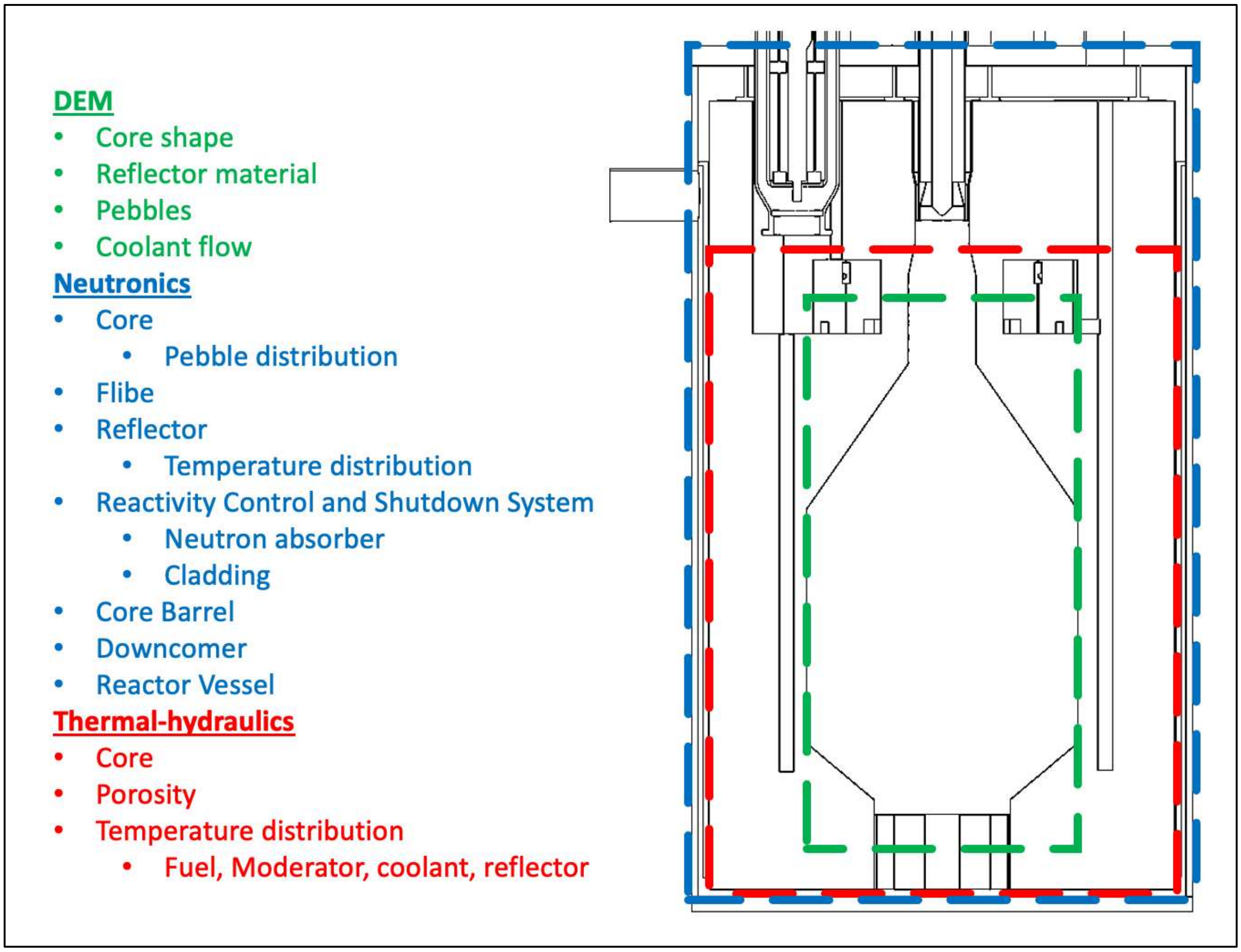

Figure 3-2 Integral TH modeling domains framework

[[

]]

Figure 3-3 Pebble Boundaries Used in the Porous Media Model

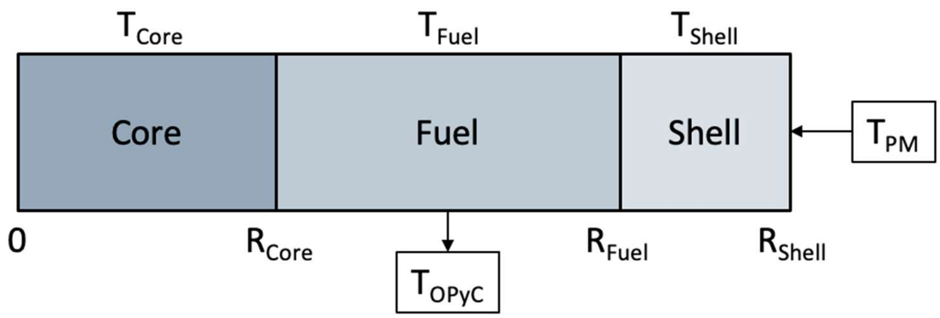

Figure 3-4 TRISO Boundaries Used in the Porous Media Model

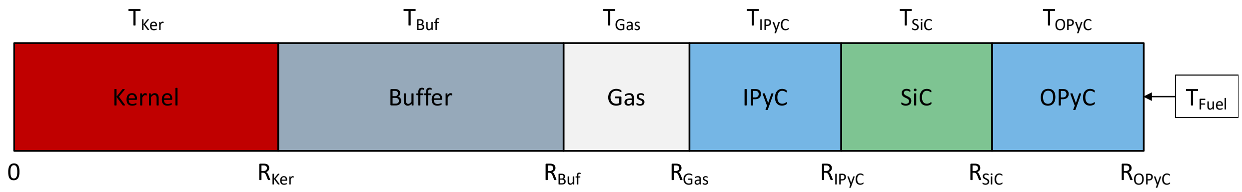

4 MODELING TOOLS

The software discussed in this report is developed and maintained under the Kairos Power Quality Assurance (QA) program, which is based on industry standard methods.

Software verification aims to ensures that the discretized model is an accurate representation of the continuous mathematical model, and that there are no user-defined code errors. Verification is performed on STAR-CCM+, Serpent 2, and the wrapper codes.

Validation is the process of determining the degree to which a mathematical model is an accurate representation of the real world from the perspective of its intended use. This is done by comparing the model outputs (FOMs) with experimental measurements and/or higher order numerical results. Validation is only performed for STAR-CCM+ and Serpent 2 because these are the underlying software codes that are used to perform the reactor physics and thermal hydraulic analysis. The wrapper codes are only used to process and exchange data between STAR-CCM+ and Serpent 2 and the libraries. The verification process consists of software benchmarking and numerical solution verification, and is described further in Section 5.

The section below introduces the software tools as they relate to the core design and analysis methodology DEM, neutronic and thermal hydraulic models, data exchange between codes, and the FOMs generated for a KP-FHR test reactor and power reactor. More detailed code descriptions are provided for STAR-CCM+ and Serpent 2 as they are the main drivers for the methodology. The other codes are used to process and transfer information between the codes and do not explicitly model core physics.

4.1 Process Flow

The KP-FHR steady state and pseudo-steady state (i.e., in the case of pebble motion) core design modeling workflow and data exchange consists of different degrees of coupling between DEM, neutronics, and TH modules. Figure 4-1 presents a graphical summary of the data flow and processing of the core modeling paradigm.

The first step in the methodology is to generate the randomly packed pebble bed core geometry. DEM modeling provides the coordinates of pebbles. TRISO particle distributions are randomized within the fuel region of pebbles. The DEM model provides all the data necessary to account for pebble residence time profiles. The neutronics module then uses the geometrical and pebble bed motion data provided by the DEM to build the core geometry and spectral zone discretization for criticality and burnup calculations. The thermal hydraulic module uses the pebble packing fraction from DEM, material and geometry inputs and operating conditions to inform the TH model. The neutronics and TH models are coupled (one-way and two-way) by power and temperature distributions to provide thermal hydraulic feedback.

4.2 STAR-CCM+

STAR-CCM+ is used for DEM and TH modeling. STAR-CCM+ is a multi-physics computational fluid dynamics simulation code. STAR-CCM+ models fluid flow and heat transfer, as well as heat transfer in solids, for complex three-dimensional geometries. It solves the Navier-Stokes equations discretized using the finite volume approach for steady state and time-dependent problems. STAR-CCM+ is used represent solid, liquid, and porous media. Heat may be transferred via conduction, and convection. As described in Section 5, the verification, validation (V&V) and uncertainty quantification methodology reduces and controls the sources of error and uncertainty between STAR-CCM+ models used in core design and their predictive capabilities. The V&V methods for DEM and TH are provided in Section 5. The TH V&V methodology focuses on the prediction of the core material temperatures (reflector, fuel, moderator, and coolant) whereas the DEM methodology focuses on the pebble center locations and their residence time profiles within the core. Kairos Power made no modifications to the base STAR-CCM+ code.

4.3 Serpent 2

Serpent 2 (Reference 39) is the main neutronics tool for reactor core design, input into safety analysis, fuel performance, and source term calculations. Serpent 2 has been extensively used across academia and industry and has been validated against various benchmarks. It is used in KP-FHR nuclear design for a variety of calculations, including multiplication factor, control and shutdown element worths, reactivity coefficients, power distribution, kinetics parameters, nuclear heating, burnup calculations, and activation analysis (see Section 3.6). Kairos Power made no modifications to the base Serpent 2 code.

4.3.1 Geometry and Particle Tracking

Serpent 2 uses a three-dimensional constructive solid geometry (CSG) model for its basic geometry routine, which is a common choice in Monte Carlo particle transport codes. The model is built using quadratic and derived surface types, forming two- or three-dimensional cells. It allows for hierarchical structuring through universes, transformations, and repeated structures like square and hexagonal lattices. A stochastic geometry model is available for handling randomly distributed fuel particle for TRISO and pebble modeling, with individual fuel particle/pebble coordinates read from a separate input file (generated using the DEM model as described in Section 3.3). Particle tracking in Serpent 2 combines conventional ray-tracing surface tracking with the rejection sampling-based delta-tracking method. Delta-tracking is useful in reactor calculations due to the typically long neutron mean-free-path compared to spatial dimensions, which results in a significant speed-up. In cases of localized heavy absorbers causing efficiency issues, the transport routine switches to surface-tracking. Delta-tracking in Serpent 2 requires that collision estimators be used for flux tallies and reaction rate integrals. The efficiency of delta-tracking in geometries with many surfaces enables Serpent 2 to model the KP-FHR with explicit pebble and TRISO particle definitions instead of approximations.

4.3.2 Interactions

Serpent 2 uses continuous-energy ACE or A Compact ENDF format cross section libraries to read neutron interaction data, serving as the foundation for the laws of physics in transport simulations. This format was originally developed for MCNP and now being leveraged by other MC tools such as OpenMC and Geant4. The software supports the use of separate thermal scattering data for moderator materials, includes probability table sampling in the unresolved resonance region, and enables the adjustment of nuclide temperatures through a built-in Doppler-broadening preprocessor routine. Additionally, the Doppler-broadening Rejection Correction (DBRC) method is employed to account for the temperature dependence of resonant scattering kernels.

Serpent 2 allows reconstruction of all cross sections using a unified energy grid. There are two benefits to using this option. First, the energy grid search required for interpolating microscopic cross sections is achieved only once for each neutron scattering event to a new energy, which reduces calculation time. Secondly, pre-calculation of material-wise macroscopic cross-sections minimize the need for summation over constituent nuclides during transport simulations, which enhances computational efficiency. Photon transport capabilities, including fission energy deposition distribution are added functionalities in Serpent 2. These capabilities are also used in modeling KP-FHRs and demonstrated in the validation, verification, and uncertainty analysis process and described in Section 5.2.

4.3.3 Burnup

Burnup calculations in Serpent 2 rely on internal subroutines, independent of external depletion solvers. The software automatically calculates decay and transmutation paths and selects nuclides for calculation without input from the user. The software gets radioactive decay data, energy-dependent fission yields, and isomeric branching ratios for neutron reactions from ENDF format data libraries.

The evolution of material undergoing depletion or burnup radioactive materials under neutron flux is described by the Bateman equation. The differential equation describing the rate of change for a single nuclide is given by the following equation (Reference 40):

$$\frac{dN_j}{dt} = -\lambda_j N_j + \sum_{i \neq j} \lambda_{ij} N_i \tag{38}$$

where N_j is the concentration of nuclide j, λ_j is the decay constant for nuclide j and λ_{ij} is the coefficients defining radioactive decay and rates of removal or addition by neutron-induced reactions.

During transport simulations, one-group transmutation cross sections, essential for the Bateman depletion equations, are calculated in real time. This method of spectrum collapsing is also used in other Monte Carlo burnup calculation codes. The irradiation history is split into different intervals with different normalizations based on power, power density, total flux, fission, or source rate. Depletion steps, for time or burnup steps, can be carried out using conventional Euler and predictor–corrector methods with linear interpolation, or more advanced techniques involving linear and quadratic interpolation and extrapolation.

In Serpent 2, the solution to the Bateman depletion equations is determined through the Chebyshev Rational Approximation Method (CRAM) matrix exponential method (Reference 41). This method provides solutions for complete nuclide systems without approximations for short-lived isotopes and limitations on step length. The method also has minimal numerical precision issues, and its accuracy and efficiency has been demonstrated to be suitable for burnup calculations which are characterized by a high number of nuclides and depletion zones. A comprehensive study of this is demonstrated by Isotalo and Aarnio in Reference 42.

4.4 Wrapper Codes

The following wrapper codes are used to transfer information between the neutronic and thermal-hydraulic codes. Wrapper codes perform data transfer and do not contain physical models that need to be validated, however their integral functions are verified.

4.4.1 HEEDS

The HEEDS code is a design and analyses software that provides tools that encompass sensitivity analyses. HEEDS couples with STAR-CCM+ and is used to perform input sensitivity and uncertainty analyses. The sensitivity analysis can be configured with a baseline STAR-CCM+ simulation from which inputs and outputs can be selected from various parameters, field functions, reports, and monitors. The inputs are parametrized with a baseline value as well as an uncertainty distribution.

4.4.2 KACEGEN

KACEGEN (Kairos ACE GENerator) is a wrapper tool developed to drive NJOY21 to produce ACE-format nuclear data libraries for use in Serpent 2 and/or MCNP6.2. NJOY21 (Reference 43) is a nuclear data processing tool capable of producing both pointwise and multi-group cross section data from the U.S. Evaluated Nuclear Data Files (ENDF) format. KACEGEN can generate ACE libraries from any ENDF-6 format library. Kairos Power has generated several libraries, including JEFF 3.3, ENDF-B-VII.1, and ENDF-B-VIII.0. Both neutron cross-sections and thermal-scattering libraries are produced for each isotope available in the library, and thermal-scattering libraries can be discrete or continuous in energy (continuous only for ENDF-B-VIII). [[

]]

4.4.3 KPACS

KPACS is an internally developed core design and analysis wrapper code that simulates the pseudo steady-state evolution of the KP-FHR core by loosely coupling Serpent 2 and discrete element modeling (DEM) in STAR-CCM+. KPACS is specifically designed to operate in two modes.

[[

]]

[[

]]

4.4.3.1 Zoner

[[

]]

4.4.4 KPATH

KPATH is the Kairos Power-developed data transfer interface that connects STAR-CCM+ to Serpent 2.
[[

]]

4.5 SCALE

The SCALE (Standardized Computer Analysis for Licensing Evaluation) code, developed by Oak Ridge National Laboratory (ORNL) (Reference 46), is a comprehensive suite of tools designed for nuclear reactor physics and radiation shielding analyses. The code includes a diverse range of modules, each tailored for specific applications, including lattice physics, burnup analysis, criticality safety, and radiation shielding. SCALE uses a vast library of nuclear data and cross-section data sets, providing accurate representations for various materials and isotopes. The code is widely used in the nuclear industry for reactor design, safety evaluations, and licensing assessments. SCALE also includes specialized modules such as TSUNAMI for sensitivity and uncertainty analysis, allowing users to assess the impact of input parameter uncertainties on FOMs. The Sampler module further enhances the capabilities of SCALE by providing a framework for generating covariance data and creating perturbed cross-section libraries for uncertainty quantification studies. The Sampler module also allows perturbation of input parameters, thereby making it a suitable framework for systems under development (i.e., KP-FHR) to investigate large parameter space. When as-built data becomes available, the module can also confirm or update calculations. Further discussion on uncertainty analysis framework and utilization of SCALE for this methodology is described in Section 5.2.

4.6 Software Quality

The software and computer codes used in the methodology described in this topical report are maintained under the Kairos Power software quality assurance program. The activities managed under the program include change management of the software and computer codes to evaluate impacts of updates and improvements along with error reporting and corrective action.

Figure 4-1 High Level Process Flow Diagram of the Core Design and Analysis Methods

[[

]]

Figure 4-2 KPACS Data Flow Diagram

[[

]]

Figure 4-3 Example of Zoner Generated Spectral Zones Used for the KP-FHR Core

[[

]]

Figure 4-4 KPATH Framework

[[

]]

5 VALIDATION, VERIFICATION, AND UNCERTAINTY ANALYSIS

This section discusses the validation, verification, and uncertainty quantification of the discrete element methodology (Section 5.1), neutronics methods (Section 5.2), and thermal hydraulic methods (Section 5.3). The verification of the neutronic methods described in this section is an inherent part of the implementation of software quality assurance (Section 4.6). The use of nuclear reliability factors (NRFs) for neutronics only applies to those FOMs used as input into safety analysis as summarized in Section 3.6. This section also includes a discussion of the method for updating neutronic uncertainties (Section 5.4) as additional operational measurements are obtained.

The overall approach for validation of the discrete element modeling, neutronics, and thermal hydraulics methods is summarized by four strategies within the methodology: 1) use state-of-the-art high fidelity computer codes, 2) benchmark these codes against other high-fidelity codes, 3) apply conservative uncertainties, and 4) confirm the validation during the startup of the test reactor. These methods are detailed in the following sections.

5.1 Discrete Element Method (DEM)

[[

]]

[[

]]

5.2 Neutronics

[[

]]

[[

]]

5.2.1 Serpent 2 Code to Code Benchmarking

[[

]]

[[

]]

5.2.1.1 Simplified KP-FHR model

[[

]]

5.2.1.2 Serpent 2 Code to Code Comparison [[ ]]

[[

]]

5.2.1.3 Criticality

[[

]]

5.2.1.4 Reactivity Coefficients

[[

]]

5.2.1.5 Fission Reaction Rates

[[

]]

5.2.1.6 Power Distribution

[[

]]

[[

]]

5.2.1.7 Rod Worth

[[

]]

5.2.1.8 Kinetics Parameters

[[

]]

5.2.1.9 Flux Distribution

[[

]]

5.2.1.10 External Source Mode

[[

]]

5.2.2 Serpent 2 Code to Code Comparison [[ ]]

[[

]]

5.2.2.1 Criticality

[[

]]

5.2.2.2 Reactivity Coefficients

[[

]]

[[

]]

5.2.2.3 Power Distribution

[[

]]

5.2.2.4 Rod Worth

[[

]]

5.2.2.5 Burnup

[[

]]

5.2.3 Uncertainty Quantification

[[

]]

[[

]]

5.2.3.1 SCALE/Sampler Certainty Tool

[[

]]

5.2.3.2 Input Uncertainty

[[

]]

5.2.3.3 Numerical Uncertainties

[[

]]

5.2.3.4 Other Sources of Uncertainty

[[

]]

5.2.4 Bias

[[

]]

5.2.4.1 Comparison to Experimental Benchmarks

[[

]]

[[
]]

5.2.4.2 Applying Modeling Bias

[[
]]

5.2.5 Margin and Nuclear Reliability Factors

[[
]]

[[

]]

5.3 Thermal-Hydraulics

This section describes the core thermal hydraulics model validation, verification, and an assessment of uncertainties [[

]]

5.3.1 Model Validation

[[

]]

[[

]]

5.3.2 Uncertainties Quantification

[[

]]

5.3.3 Model Validation [[ ]]

[[

]]

[[

]]

5.3.4 Numerical Error and Solution Verification

[[

]]

5.3.5 Input Uncertainties

[[

]]

[[ ]]

5.3.6 Modeling Biases and Confidence Level Factors

[[

]]

5.3.7 KP-FHR Testing

KP-FHR test reactor will provide temperature measurements of reflector graphite, core outlet, reactor inlet and outlet to confirm the proposed methodology uncertainty assessment.

5.4 Methodology for Updating NRFs With Operational Data

[[

]]

[[

]]

5.5 Validation, Verification and Uncertainty Analysis Summary

The preceding sections have described the methodology for verification, validation, and uncertainty quantification for the DEM, neutronics, and thermal hydraulics methods for analysis of a KP-FHR.

The validation methodology for DEM is performed by [[

]]

A method for updating the nuclear reliability factors is described in section 5.4, which relies on use of measure data from KP-FHR reactor operation. [[

]]

Table 5-1 Parameters for Code-to-Code Benchmark [[ ]]

[[

]]

[[

]]

Table 5-2 V&V Model Naming Convention

[[

]]

Table 5-3 Summary of Methodology for Code-to-Code Benchmark Parameters [[ ]]

[[

]]

[[

]]

Table 5-4 Comparison of Multiplication Factor [[ ]]

[[

]]

Table 5-5 Comparison of Calculated ITCs [[ ]]

[[

]]

Table 5-6 Comparison of Calculated CVCs [[ ]]

[[

]]

Table 5-7 Comparison of Calculated CTCs [[ ]]

[[

]]

Table 5-8 Comparison of Calculated FTCs [[ ]]

[[

]]

Table 5-9 Comparison of Calculated MTCs [[ ]]

[[

]]

Table 5-10 Comparison of Calculated RTCs [[ ]]

[[

]]

Table 5-11 RCS Total Bank Worth Calculations [[ ]]

[[

]]

Table 5-12 Calculated [[ ]] Six-Group Delayed Neutron Yield

[[

]]

Table 5-13 Calculated [[ ]] Six-Group Delayed Neutron Time Constants

[[

]]

Table 5-14 ESM Detector Calculations for Reflector Regions *(subcritical case 1)*

[[

]]

Table 5-15 ESM Detector Calculations for Reflector Regions *(subcritical case 2)*

[[

]]

Table 5-16 Comparison of Multiplication Factor [[ ]]

[[

]]

Table 5-17 Comparison of Calculated ITCs

[[

]]

Table 5-18 Comparison of Calculated CVCs

[[

]]

Table 5-19 Comparison of Calculated CTCs

[[

]]

Table 5-20 Comparison of Calculated FTCs

[[

]]

Table 5-21 Comparison of Calculated MTCs

[[

]]

Table 5-22 Comparison of Calculated RTCs

[[

]]

Table 5-23 RCS Total Bank Worth Calculations

[[

]]

Table 5-24 Summary of [[ ]] Components and Nuclear Data for Code-to-Code Burnup Comparison

[[

]]

Table 5-25 Benchmarked Experiments Used for Bias Estimation

[[

]]

Table 5-26 Bias Corrections

[[

]]

Table 5-27 Sources of Unquantified Uncertainty

[[

]]

Figure 5-1 COF Calibration Phase 1 Sensitivity Analysis

[[

]]

Figure 5-2 COF Calibration Phase 2 Fully Packed Core

[[

]]

Figure 5-3 Simplification for sKPH Model

[[

]]

Figure 5-4 1-D Axial Fission Rate Distribution Comparison [[ ]]

[[

]]

Figure 5-5 1-D Radial Fission Rate Distribution Profile Comparison [[ ]]

[[

]]

Figure 5-6 Integral Bank Worth Comparison [[ ]]

[[

]]

Figure 5-7 Differential Bank Worth Comparison [[ ]]

[[

]]

Figure 5-8 Integral RCS Bank Worth [[ ]] Results Comparison

[[

]]

Figure 5-9 Differential RCS Bank Worth [[ ]] Results Comparison

[[

]]

Figure 5-10 Burnup Comparison [[ ]] for Single Fuel Pebble Depletion in Pebble Zone R0Z0

[[

]]

Figure 5-11 Burnup Comparison [[ ]] for Single Fuel Pebble Depletion in Pebble Zone R2Z1

[[

]]

Figure 5-12 Nuclear Uncertainty Quantification

[[

]]

Figure 5-13 Geometrical Features of the High-Fidelity Packed Bed Model

[[

]]

Figure 5-14 Porous Media Validation Framework

[[

]]

6 APPLICATIONS

This section provides an overall description of the calculational methodology that are used within the core design codes and models described in Sections 3 and 4 of this topical report. This section also provides a description of the core physics parameters, which are used in downstream applications and as inputs into safety analysis, source term, and nuclear design.

6.1 Input into Safety Analysis

For neutronic parameters, enough cycles and histories per cycle must be run to, at a minimum, guarantee the convergence of the fission source distribution (i.e., Shannon entropy). However, an increased number of runs are used depending on the required rigor of the FOM for downstream applications. The Monte Carlo (MC) error is expected to be small relative to the uncertainty in FOMs calculated using methodologies described in Section 5.

6.1.1 Reactivity Coefficients

The calculations for reactivity coefficients are performed using Equation 51:

$$\alpha_x = \frac{\rho_{\Delta\mathrm{x}} - \rho_{ref}}{\Delta x} = \frac{1}{\Delta x}\left(\frac{1}{k_{ref}} - \frac{1}{k_{\Delta x}}\right) \tag{51}$$

where α_x is the reactivity coefficient with respect to quantity *x,* Δx is the change in quantity *x* with respect to a reference condition (positive or negative), k_{ref} is the neutron multiplication factor of the core calculated from Serpent 2 at reference conditions, and $k_{\Delta x}$ is the neutron multiplication factor of the core calculated by Serpent 2 after *x* was changed by Δx. The KP-FHR reactivity feedback includes fuel temperature, coolant temperature, coolant void, moderator temperature, and reflector temperature as well as the isothermal temperature coefficient.

The fuel temperature coefficient (FTC), or Doppler coefficient, is calculated by changing the fuel kernel temperature. The coolant temperature coefficient (CTC) is calculated by changing the Flibe temperature and associated density. The Flibe temperature only changes in the pebble bed region, downcomer, core barrel gap, defueling region, and upper and lower plenum when there is a change to the coolant temperature coefficient. The coolant void coefficient (CVC) is calculated by changing the Flibe density in the same Flibe components as in the CTC calculation. Moderator temperature coefficient (MTC) is calculated by changing the temperature of all non-fuel material within the pebbles of the core (i.e., buffer, IPyC, SiC OPyC, pebble fuel matrix, pebble core, pebble shell, and the graphite pebbles). The reflector temperature coefficient (RTC) is calculated by changing the entire graphite reflector temperature (i.e., top, bottom, and side reflector) and does not account for change in temperature dependent Flibe density. The isothermal temperature coefficient (ITC) is calculated by homogeneously varying the temperatures of the fuel, coolant, moderator, and reflector.

6.1.2 Rod Worth

The reactivity shutdown system (RSS) design provides adequate reactivity worth to compensate for the following:

- Positive reactivity inserted from the decay of full power xenon
- Change in temperature from full-power conditions to safe shutdown temperature (i.e., power defect)
- Maximum operational excess reactivity

- Highest worth stuck element (i.e., fully withdrawn)
- Uncertainties, [[

]]

The maximum operational excess reactivity (which is controlled by the total fuel loading) is the additional reactivity available to the reactor and is used to change power levels or manage other transients such as a change in the mass flow rate, inlet coolant temperature, or depletion of absorber in the Flibe or reflector. The value of maximum operational excess reactivity is set for all core states. Element insertion limits will be defined, as needed.

[[

]] The control elements in the RCS are responsible for all planned, normal power maneuvers. The worth requirements depend on the KP-FHR design.

Rod worth is calculated using Equation 52 where $k_{eff,out}$ is the withdrawn position and $k_{eff,in}$ is the inserted position of interest. Differential control worth is calculated using Equation 53, where $k_{eff,i}$ is the neutron multiplication factor of the core for the control rod(s) position at step i, $k_{eff,i+1}$ is the neutron multiplication factor of the core for the control rod(s) position at step $i+1$, z_i is the axial position of the control rod(s) at step i, and z_{i+1} is the axial position of the control rod(s) at step $i+1$.

[[

]]

6.1.3 Neutron Kinetics Parameters

In addition to reactivity coefficients, kinetics parameters such as delayed neutron fraction and their associated decay constant(s), neutron mean generation time, and neutron mean lifetime are also calculated and provided as input into safety analysis. The kinetics parameters are calculated using the iterated fission probability method (Reference 59) of Serpent 2.

Delayed photoneutrons, from Be (γ, n) reaction in Flibe, are also assessed to understand their impact on the effective delayed neutron fraction and delayed neutron group structure (Reference 60). This impact from delayed photoneutrons is smaller than other reactors (i.e., heavy water reactors) that have been impacted from this source of delayed neutrons.

6.1.3.1 Application of Bias

Kinetics parameters are obtained from Serpent 2 and used in the point kinetics model for safety analysis. Serpent 2, similar to MCNP6.2, uses adjoint weighted method to calculate these parameters, including delayed neutron fraction (β_{eff}) and prompt neutron lifetime (l_p). The results from Serpent 2 are verified using calculations of β_{eff} and l_p through the prompt method and the 1/ v insertion method respectively (Reference 61). For verifying the prompt method calculation, β_{eff} is calculated using Equation 54:

$$\beta_{eff} = 1 - k_p * k^{-1} \tag{54}$$

where k_p is the prompt neutron multiplication factor and k is the multiplication factor for all neutrons in the system. The 1/ v insertion method calculates the prompt neutron lifetime represented as l_p in Equation 55:

$$l_p = \frac{1}{N_{B-10}\sigma_{a0}v_0}\frac{k_{ref} - k_p}{k_p} \tag{55}$$

where k_{ref} is the eigenvalue of the original system, k_p is the eigenvalue of the system with trace amounts of B-10, N_{B-1} is the boron-10 number density in atoms/(barn-cm), v_0 is 220,000 cm/s, and σ_{a0} is 3837 barns at 220,000 cm/s. Kinetics parameters are dependent on the response time (e.g., at startup core and equilibrium core compositions), as well as the isotopic composition of the fission products when an equilibrium core is reached.

6.1.4 Power Distribution

Core methodology provides power distributions inside the vessel region. Table 3-5 summarizes the powers that are provided by the methodology inside the vessel. Table 6-1 describes the format, and Tables 6-2, 6-3, and 6-4 provide definitions of power peaking factors. [[

]]

6.1.5 Depletion Calculations

6.1.5.1 Fuel Cycle

KPACS, as described in Section 4.4.3, is used to calculate different core composition states (i.e., equilibrium and transition core). To sustain the desired level of under-moderation while maintaining acceptable excess reactivity, pebble bed reactors start with an initial composition that is a combination of lower enriched fuel (down to depleted uranium) and higher enriched fuel. The transition core is the state between initial core composition and final equilibrium core composition and starts by first removing lower enriched fuel and replacing by the higher enriched fuel. KPACS analyzes core composition at various time steps. The spectrum in the core evolves as the core composition progresses towards equilibrium. Operation within the boundaries set by excess reactivity (i.e., accounting for rod insertion limits, if applicable) ensures that the operational and safety-related parameters of transition core states are bounded by the end states (i.e., low-power and equilibrium cores).

6.1.5.2 General Depletion

[[

]]

6.1.6 Spectrum Averaged Cross Sections

[[

]]

6.2 Inputs into Nuclear Design

The tools used in Section 4 are used to provide input parameters in the areas identified in this section.

6.2.1 Sources of Reactivity

The evolution of Flibe and the structural graphite throughout the operational lifetime of a KP-FHR reactor has an impact on core reactivity, reactivity coefficients, and the neutron spectrum, which are used in the safety analysis. The presence of Li-6 and other impurities present in fresh Flibe and graphite at startup, as well as the addition of corrosion products, are considered in core modeling. Serpent 2 allows material definitions to be inserted and burnup analysis to be performed for relevant materials.

6.2.2 Flux Distribution

Neutron and gamma flux and associated spectrums are a direct output of Serpent 2 MC radiation transport simulations that use appropriate tallies. Distribution of neutron and gamma flux within the reactor vessel has secondary applications, such as power distribution calculations, cross section averaging, fluence to vessel internals, displacement per atom (DPA) calculations, and other similar applications. This capability is a direct derivative of defined tallies in Serpent 2 with appropriate energy structure.

6.2.3 Radiation Fluence on the Vessel and Internals and Radiation Damage

Serpent 2 is used to calculate the fast neutron fluence on the vessel and the internals, including but not limited to core barrel, pebble insertion line, graphite reflector, RCS, and RSS. Serpent 2 is also used to calculate helium (alpha) generation in the vessel and other metallic components within the vessel.

[[

]]

6.2.4 Power Distribution

[[

]]

6.2.5 Nuclear Stability

KP-FHRs are characterized by their high-power density. The fundamental design features of a KP-FHR (described in Section 2.1) result in a large neutron diffusion length (L) and neutron migration area (M), which are calculated using Serpent 2. [[

]]

6.3 Thermal Hydraulics

The two major applications of the core thermal hydraulics methodology are 1) characterization of core and reflector material temperatures for cross sections and 2) qualification boundaries for fuel and reflector graphite temperatures.

6.3.1 Core Temperatures

[[

]]

6.3.2 Reflector Temperatures

[[

]]

6.4 Core Composition

[[

]]

6.5 Core Follow

The tools described in Section 4 are used to predict reactor physics parameters for KP-FHR reactors during operation, encompassing the continuous refueling and burnup of fuel and Flibe, as the core undergoes evolution. The methodology provided in this report is used to account for the operational history (i.e., power and inserted pebble histories) and provides the predicted core composition. At a minimum, the comparison of the rod position is compared against predictions.

6.6 Startup Physics Testing

The startup process of a KP-FHR consists of two phases: fuel loading and zero power testing. The fuel loading process is the process in which a combination of fuel and moderator pebbles are loaded incrementally into the core. The first two steps of this process rely on the critical mass predictions using Serpent 2 and associated uncertainties. The first two insertions of fissile content into the core are limited to less than 50% of the lower bound of the critical loading estimate. Until the core achieves criticality, the process will use the 1/M approach for each step's prediction. The process of performing zero-power testing includes control rod calibration, shutdown rod worth, and isothermal temperature coefficient measurements are performed and are compared against predictions. If, during startup physics testing, predicted values with added uncertainties do not align with measured data, testing will be suspended. The impact on the safety analysis due to potential changes in nuclear reliability factor applicability will be evaluated before testing is resumed.

Once all zero-power physics testing is successfully completed, power ascension begins. Measurements of important reactor physics parameters will be repeated at designated hold points during power ascension, including but not limited to shutdown rod worth and control rod worth.

Table 6-1 Power Format and Description

[[

]]

Table 6-2 Global Peaking Factor

[[

]]

Table 6-3 Axial Peaking Factor

[[

]]

Table 6-4 Radial Peaking Factor

[[

]]

Figure 6-1 Core Composition Uncertainty Analyses

[[

]]

7 SUMMARY

An analysis method consisting of Serpent 2, STAR-CCM+, and the calculational framework associated with the codes described in Section 4 support the neutronics and thermal hydraulic design, steady-state analysis, and licensing of KP-FHRs. The software quality assurance program at Kairos Power is an integral part of the development and maintenance of this analysis framework.

The neutronics portion of this methodology relies on Serpent 2. [[

]] Additionally, such predictions will be confirmed during the fuel loading process and subsequent zero-power testing of Hermes and future KP-FHRs.

The thermal-hydraulics portion of this methodology produces temperature distributions across the vessel, including pebble bed and reflector geometry for a defined boundary. [[

]]

Both code-qualifying approaches (described in Section 5.2 and 5.3 for neutronics and thermal hydraulics respectively), are applicable to different KP-FHRs, given that the proper range of applicability is applied to the benchmarking methodology.

7.1 Conclusions

The DEM methodology described in Section 3.3 of this topical report is acceptable for generating both a random packed pebble bed and TRISO distributions to use for a Serpent 2 baseline model geometry (Section 3.4) in thermal hydraulic validation benchmarks. These benchmarks, described in Section 5.3, are then used to inform the porous media models described in Section 3.5. This methodology is also able to adequately predict pebble tracks and velocity profiles during pebble recirculation. Pebble tracks and velocity profiles are used to generate core spectral zone boundaries for the fuel cycle analysis tool, KPACS, using Zoner (Section 4.4.3.1).

The method for using bounding DEM sensitivity analyses to assess the effect of COF on DEM models and predict the impact on FOMs is adequate for use in a KP-FHR. The sensitivity range is informed by internal tribology testing representative of the KP-FHR core conditions. During reactor startup physics testing, the DEM-COF calibration with respect to total number of pebbles in a fully packed core is performed. The final calibrated COF is used as baseline input for the DEM contact force model.

The thermal hydraulics methodology (described in Section 3.5) that is used to predict core material temperature distribution for Flibe, graphite pebbles, fuel pebble layers, TRISO layers, and reflector temperature distribution for applications described in Section 6.3 is also an adequate methodology for a KP-FHR. Predicted temperature values are used to model reactor temperature feedback in Serpent 2 models.

[[

]]

The conservative nuclear reliability factors (NRFs) for the neutronics FOMs are determined using quantifiable uncertainties, bias derived from similar systems (see Table 5-26) and discretionary conservatism (see Table 5-27).

Based on these conclusions, this topical report provides an acceptable methodology for core design and analysis subject to the limitations in Section 7.2.

7.2 Limitations

Modeling tools and methods described in this topical report are applicable to KP-FHR steady-state operation. The methodology limitations include the applicability of the correlations used in the thermal-hydraulics modeling of the core.

This core design and analysis methodology is subject to the following limitations:

1. The methodology described is applicable to a KP-FHR consistent with the design described in Section 1.1.
2. The methodology is applicable to steady-state conditions.
3. Application of the methodology for future KP-FHRs will use measured data including isothermal temperature reactivity coefficient and the shutdown worth from a KP-FHR test reactor, to update nuclear reliability factors.
4. The confidence level factor and bias for thermal hydraulic figures of merit are limited to KP-FHR test reactors. Use in power reactors will be justified using applicable separate effects tests or measured data from a KP-FHR test reactor.
5. If discretionary conservatisms provided in Table 5-27, are updated for use in future KP-FHRs beyond Hermes, new discretionary conservatisms must be justified by KP-FHR measurement data.
6. Ranges of applicability of the [[ ]] are determined by the methodology provided in Section 5.3.
7. The pebble velocity needs to be a small fraction of the time constant of delayed neutron precursors.
8. The software and computer codes used are maintained under the Kairos Power software quality assurance program.

8 REFERENCES

1. Kairos Power LLC, "Principal Design Criteria for the Kairos Power Fluoride Salt-Cooled High Temperature Reactor," KP-TR-003-P-A, Revision 1, July 2019.
2. D. Diamond, C. Edgar, M. Fratoni, H. Gougar, A. Hawari, J. Hu, N. Hudson, D. Ilas, I. Maldonado, B. Petrovic, F. Rahnema, D. Serghiuta and D. Zhang, "Phenomena Identification and Ranking Tables (PIRT) Report for Flourid High-Temperature Reactor (FHR) Neutronics," Transactions of the American Nuclear Society, 2016.
3. Johnson, K.L “Contact Mechanics,” 1987 Cambridge University Press, Cambridge.
4. Di Renzo, Alberto and Di Maio, Francesco Paolo. 2004. “Comparison of contact-force models for the simulation of collisions in DEM-based granular flow codes,” Chemical Engineering Science 59 pp. 525-541.
5. Laufer, M. R. “Granular Dynamics in Pebble Bed Reactor Cores,” UC Berkeley, 2013.
6. Gidaspow, D., 1994. “Multiphase flow and fluidization: continuum and kinetic theory descriptions.”
7. Nuclear Safety Standards Commission. Reactor Core Design of High-Temperature Gas-Cooled Reactors; Part 3: Loss of Pressure through Friction in Pebble Bed Cores. Technical Report. KTA 3102.2 1987; Issue 3/81.
8. K. Wakao, S. Kaguei and T. Funazkri, "Effect of fluid dispersion coefficients on particle-to-fluid heat transfer coefficients in packed beds," Chemical Engineering Science, vol. 34, pp. 325-326, 1978.
9. S. Yagi and N. Wakao, "Heat and mass transfer from wall to fluid in packed beds," A.I.Ch.E., vol. 5, no. 1, pp. 79-85, 1959.
10. Hu, G., O'Grady, D., Zou, L. and Hu, R., 2020. Development of a Reference Model for Molten-Salt-Cooled Pebble-Bed Reactor Using SAM (No. ANL/NSE-20/31). Argonne National Lab.
11. Kairos Power LLC, "Reactor Coolant for the Kairos Power Fluoride Salt-Cooled, High Temperature Reactor," KP-TR-005-P-A, Revision 1, January 2020.
12. Novak, A.J., Schunert S., Carlsen R.W., Balestra P., Andrs D., Kelly J., Slaybaug R.N., Martineau R.C., H.D., 2020. Pronghorn theory manual (No. INL/EXT-18-44453-Rev001). Idaho National Lab
13. Stainsby, R., Grief, A., Worsley, M. and Dawson, F., 2009. Investigation of local heat transfer phenomena in a pebble bed HTGR core. AMEC NSS Limited, London, United Kingdom.
14. Novak, A.J., Schunert, S., Carlsen, R.W., Balestra, P., Slaybaugh, R.N. and Martineau, R.C., 2021. Multiscale thermal-hydraulic modeling of the pebble bed fluoride-salt-cooled high-temperature reactor. Annals of Nuclear Energy, 154, p.107968.
15. Sen, R.S. and Viljoen, C.F., 2012. The re-evaluation of the AVR melt-wire experiment with specific focus on different modeling strategies and simplifications. Nuclear engineering and design, 251, pp.306-316.
16. van Rensburg, J.J. and Kleingeld, M., 2011. CFD applications in the Pebble Bed Modular Reactor Project: A decade of progress. Nuclear engineering and design, 241(9), pp.3683-3696.
17. Nield, Donald A and Adrian Bejan, “Convection in Porous Media,” Vol 3, 2006.
18. Satvat, N., Sarikurt, F., Johnson, K., Kolaja, I., Fratoni, M., Haugh, B. and Blandford, E., 2021. Neutronics, thermal-hydraulics, and multi-physics benchmark models for a generic pebble-bed fluoride-salt-cooled high temperature reactor (FHR). Nuclear Engineering and Design, 384, p.111461.
19. Bear, J., 2013. “Dynamics of fluids in porous media.” Courier Corporation.
20. Ingham, D.B. and Pop, I., 1998. “Transport phenomena in porous media.”
21. Wakao, N. and Kagei, S., 1982. “Heat and mass transfer in packed beds” (Vol. 1).
22. Wilcox, D.C., 2006. “Turbulence modeling for CFD” (Vol. 1). La Canada, CA: DCW industries.
23. Pope, S.B., 2001. Turbulent flows. Measurement Science and Technology, 12(11), pp.2020-2021.

24. Ferziger, J.H. and Peric, M. 2002. “Computational Methods for Fluid Dynamics,” 3rd rev. ed., Springer-Verlag, Berlin.
25. Versteeg, H.K. and Malalasekera, W., 1995. Computational fluid dynamics. The finite volume method, pp.1-26.
26. Patankar, S., 2018. “Numerical heat transfer and fluid flow.” Taylor & Francis.
27. Kairos Power LLC, “Fuel Qualification Methodology for the Kairos Power Fluoride Salt-Cooled High Temperature Reactor (KP-FHR)” KP-TR-011-P-A, Revision 2, June 2022.
28. NEA (2015), Best Practice Guidelines for the Use of CFD in Nuclear Reactor Safety Applications – Revision, OECD Publishing, Paris.
29. ASME Standard for Verification and Validation in Computational Fluid Dynamics and Heat Transfer V&V 20 - 2009(R2021).
30. van Rensburg, J.J. and Kleingeld, M., 2011. An integral CFD approach for the thermal simulation of the PBMR Reactor Unit. Nuclear engineering and design, 241(8), pp.3130-3141.
31. van Rensburg, J.J. and Kleingeld, M., 2011. Investigating leakage and bypass flows in an HTR using a CFD methodology. Nuclear engineering and design, 241(12), pp.4960-4971.
32. van Rensburg, J.J. and Kleingeld, M., 2010. A CFD method to evaluate the integrated influence of leakage and bypass flows on the PBMR Reactor Unit. Nuclear engineering and design, 240(11), pp.3841-3850.
33. Jurtz, N., Kraume, M. and Wehinger, G.D., 2019. Advances in fixed-bed reactor modeling using particle-resolved computational fluid dynamics (CFD). Reviews in Chemical Engineering, 35(2), pp.139-190.
34. Dixon, A.G. and Partopour, B., 2020. Computational fluid dynamics for fixed bed reactor design. Annual review of chemical and biomolecular engineering, 11, pp.109-130.
35. Eppinger, T. and Wehinger, G.D., 2021. A Generalized Contact Modification for Fixed-Bed Reactor CFD Simulations. Chemie Ingenieur Technik, 93(1-2), pp.143-153.
36. Jurtz, N., Wehinger, G.D., Srivastava, U., Henkel, T. and Kraume, M., 2020. Validation of pressure drop prediction and bed generation of fixed-beds with complex particle shapes using discrete element method and computational fluid dynamics. AIChE Journal, 66(6), p.e16967.
37. Wang, S.W., Zhou, C., Wang, N.X., Cai, C.X., Zhu, H.H. and Zou, Y., 2024. Numerical analysis and validation on heat transfer characteristics and correlation of molten salt in pebble bed channel. Nuclear Engineering and Design, 418, p.112920.
38. Eppinger, T., Seidler, K. and Kraume, M., 2011. DEM-CFD simulations of fixed bed reactors with small tube to particle diameter ratios. Chemical Engineering Journal, 166(1), pp.324-331.
39. VTT, "Publications and reports related to Serpent development," VTT, 18 May 2021. [Online]. Available: http://montecarlo.vtt.fi/publications.htm. [Accessed 18 May 2021].
40. Pusa, M. and Leppänen, J. “Computing the matrix exponential in burnup calculations,” Nucl. Sci. Eng., 164(2010) 140-150.
41. Pusa, M. “Rational approximations to the matrix exponential in burnup calculations” Nucl. Sci Eng., 169(2011) 155-167.
42. Isotalo, A. and Aarnio, P. “Comparison of depletion algorithms for large systems of nuclides.” Ann. Nucl. Energy, 38(2011) 261-268.
43. J. L. Conlin, A. Kahler, A. P. McCartney and D. A. Rehn, "NJOY21: Next generation nuclear data processing capabilities," International Conference on Nuclear Data for Science and Technology, vol. 146, 2017.

44. H. J. Rutten, K. A. Haas, H. Brockmann, U. Ohlig, C. Pohl and W. Scherer, "VSOP (99/09) Computer Code System for Reactor Physics and Fuel Cycle Simulation; Version 2009,"Forschungszentrum, Jülich, 2009.
45. W. G. D.Bedenig, “Parameter Studies Concerning the Flow Behavior of a Pebble with Reference to the Fuel Element Movement in the Core of the THTR 300MWe Prototype Reactor,” Nuclear Engineering and Design, vol. 7, pp. 367-378, 1968.
46. W. A. Wieselquist, R. A. Lefebvre, M. A. Jessee and Eds., "SCALE Code System, ORNL/TM-2005/39, Version 6.2.4," Oak Ridge National Laboratory, Oak Ridge, TN, 2020.
47. Kairos Power LLC, “Scaling Methodology for the Kairos Power Testing Program” KP-TR-006-P-A, Revision 1, June 2020.
48. R. Tuominen, J. Leppänen and V. Valtavirta, "New energy deposition treatment in the Serpent 2 Monte Carlo transport code," Annals of Nuclear Energy, vol. 129, pp. 224-232, 2019.
49. Talamo, A., Bergeron, A., Subhasish, M., Vegendla, S. P., Heidet, F., Ade, B., & Betzler, B. (n.d.). Monte Carlo Calculation of the Energy Deposition in the Transformational Challenge Reactor. UChicago Argonne LLC.
50. Wang, X., Liu, Y., Martin, W., & Kim, K. S. (2018). Energy Deposition Analysis for VERA Progression Problems by MCNP. PHYSOR. Cancun, Mexico.
51. Chadwick, M. B., & et. al. (2006). ENDF/B-VII.0: Next Generation Evaluated Nuclear Data Library for Nuclear Science and Technology. Nuclear Data Sheets, 107(12), 2931-3060. doi:https://doi.org/10.1016/j.nds.2006.11.001
52. AMEC, Investigation of local Heat Transfer Phenomena in a Pebble Bed HTGR Core, NROOl/RP/002 ROl, May 15, 2009.
53. Owen, D.B., “Factors for One-Sided Tolerance Limits and For Variables Sampling Plans,” March 1963.
54. D. S. G. I. J. P. M. Fratoni, "Molten Salt Reactor Experiment Benchmark Evaluation (Project 16-10240)," UC Berkeley.
55. L. M. O. K. L. S. J. Bess, "Benchmark Evaluation of HTR-PROTEUS Pebble Bed Experimental Program," Nuclear Science and Engineering, vol. 178, no. 3, pp. 387-400, 2014.
56. H. H. J. O. G. S. K. V. W. Z. F. Bostelmann, "Criticality Calculations of the Very High Temperature Reactor Benchmark with Serpent and SCALE/KENO-VI," Idaho National Laboratory, April 2016.
57. F. B. G. Strydom, "Nuclear Data Uncertainty and Sensitivity Analysis of the VHTRC benchmark using SCALE," Idaho National Laboratory, December 2017.
58. S. S. Y. W. V. L. F. G. R. M. J. Ortensi, "Benchmark Analysis of the HTR-10 with the MAMMOTH Reactor Physics Application," United States: N.p., 2018 Web. doi: 10.2172/1468643.
59. J Leppänen, M Aufiero, E Fridman, R Rachamin, S Marck, "Calculation of effective point kinetics parameters in the Serpent 2 Monte Carlo code" Annals of Nuclear Energy, Volume 65, 2014, Pages 272-279, ISSN 0306-4549.
60. C. Keckler, N. Satvat, K. Johnson, B. Haugh, M. Fratoni, "Photoneutron production and characterization in fluoride-salt cooled high-temperature reactors," Nuclear Engineering and Design, Volume 372, 2021, 110976, ISSN 0029-5493.
61. University of Utah Nuclear Reactor Facility, License Renewal Application Updated Safety Analysis Report, June 2011 (ML111720666).
62. Duderstadt, J. J. and Hamilton, L.J., 1976. “Nuclear Reactor Analysis”
63. Weissberg A., and Beatty, G. H., "Tables of Tolerance-Limit Factors for Normal Distributions", Technometric, vol. 2, no. 4, 1960.

APPENDIX A. Example Calculation

Calculation results for an example Hermes design are described in this appendix to illustrate the application of the methodology described in this topical report.

A.1.1 Neutronics

[[

]]

A.1.1.1 Inputs to Safety Analysis

[[

]]

A.1.1.1.1 Reactivity Coefficients

[[

]]

A.1.1.1.2 Shutdown Margin

[[

]]

A.1.1.1.3 RCSS Total Worth

[[

]]

A.1.1.1.4 RCS Bank Integral and Differential Worth

[[

]]

A.1.1.1.5 RSS Bank Integral and Differential Worth

[[

]]

A.1.1.1.6 Kinetics Parameters

[[

]]

A.1.1.1.7 Fission Power and Flux Distributions

[[

]]

A.1.1.1.8 Power Peaking Factors

[[

]]

A.1.1.2 Demonstration of Uncertainty Analysis Tool

[[

]]

A.1.1.2.1 Input Design Space

[[

]]

A.1.1.2.2 Demonstration of Sensitivity Study

[[

]]

A.1.1.2.3 Determination of KP-FHR Core Composition Space

[[

]]

[[

]]

A.1.1.2.4 Uncertainty Quantification for Inputs to KP-FHR Inputs to Safety Analysis

[[

]]

A.1.1.3 Determining Bounds of Conservatism for Inputs to Safety Analysis Parameters

A.1.1.3.1 Nuclear Data and RSS Modeling Bias for ITC and RSS Total Worth

[[

]]

A.1.1.3.1.1 Carbon Cross-Section and Thermal Scattering Nuclear Data Bias

[[

]]

[[

]]

A.1.1.3.1.2 RSS Insertion Modeling Bias

[[

]]

A.1.1.3.2 Applying Nuclear Reliability Factors to ITC

[[

]]

A.1.1.3.3 Applying Nuclear Reliability Factors to SDM

[[

]]

A.2 Thermal Hydraulics

The thermal hydraulic example calculations are provided below reflecting the applications and figures of merit described in Section 6 of the topical report.

[[.

]]

A2.1 Core temperatures characterization

[[

]]

[[

]]

A2.2 Reflector temperatures qualification

[[

]]

Table A.1-1 Reactivity Coefficients Calculated for Hermes λ-and Ω-core States

[[

]]

Table A.1-2 Hermes λ-and Ω-Core Shutdown Margin

[[

]]

Table A.1-3 Total RCS/RSS Bank Worth

[[

]]

Table A.1-4 Hermes Kinetics Parameters for λ-and Ω-core States

[[

]]

Table A.1-5 Group-wise Delayed Neutron Fraction for λ-and Ω-core States

[[

]]

Tabel A.1-6 Group-wise Delayed Time Constant for λ-and Ω-core States

[[

]]

Table A.1-7 Material Temperature Inputs and Distributions

[[

]]

Table A.1-8 Material Density Inputs and Distributions

[[

]]

Table A.1-9 Material Impurities Input and Heavy Metal Loading Distributions

[[

]]

Table A.1-10 Uncertainty Quantification of ITC for Hermes λ-and Ω-cores

[[

]]

Table A.1-11 Uncertainty Quantification of RSS bank total worth for Hermes λ-and Ω-cores

[[

]]

Table A.1-12 Determined ITC and RSS Total Worth Nuclear Data and Modeling Biases for Hermes λ- and Ω-Cores

[[

]]

Table A.1-13 Comparison of Calculated Isothermal Temperature Coefficient for Considered Carbon Cross-Section and Thermal Scattering

[[

]]

Table A.1-14 Comparison of Calculated RSS Total Worth for Considered Carbon Cross-Section and Thermal Scattering Libraries

[[

]]

Table A.1-15 Determination of ITC Bounds of Uncertainty Based on Determination of Nuclear Reliability Factor

[[

]]

Table A.1-16 Determination of SDM Bounds of Uncertainty Based on Determination of Nuclear Reliability Factor

[[

]]

Table A.2-1 Summary of Core TH Model Biases and Uncertainties for the Zone (R1, Z3)

[[

]]

Table A.2-2 Summary of Integral TH Model Biases and Uncertainties for Peak Reflector Temperature

[[

]]

Figure A.1-1 RCS Integral Worth Curves for λ-and Ω-cores

[[

]]

Figure A.1-2 RCS Differential Worth Curves for λ-and Ω-cores

[[

]]

Figure A.1-3 RSS Integral Worth Curves for λ-and Ω-cores

[[

]]

Figure A.1-4 RSS Differential Worth Curves for λ-and Ω-cores

[[

]]

Figure A.1-5 Axial Fission Power Profile for Hermes λ-and Ω-cores Normalized Over Total Power

[[

]]

Figure A.1-6 Radial Fission Power Profile for Hermes λ-and Ω-cores Normalized Over Average Power Density

[[

]]

Figure A.1-7 Axial Flux Profile for Hermes λ-and Ω-cores Normalized Over Average Flux

[[

]]

Figure A.1-8 Radial Flux Profile for Hermes λ-and Ω-cores Normalized Over Average Flux

[[

]]

Figure A.1-9 [[ ]]

[[

]]

Figure A.1-10 Axial and Radial Power Density Peaking Factor Distributions

[[

]]

Figure A.1-11 2D Power Peaking Factor Distribution

[[

]]

Figure A.1-12 Sensitivity of Effective Multiplication Factor with Respect to Lithium-6 Concentration in Flibe, Kernel Boron and HML and Reflector Boron

[[

]]

Figure A.1-13 Sensitivity of Effective Multiplication Factor with Respect to Pebble/TRISO Boron, Reflector Density, and Flibe Density and Temperature

[[

]]

Figure A.1-14 Ranges of CVC with Respect to Flibe Lithium-6 Enrichment for Various Hermes λ-core Moderator Pebble Ratios

[[

]]

Figure A.1-15 Multiplication Factor Versus Moderator Pebble Ratio for Various Flibe Lithium-6 Concentration (optimal moderation)

[[

]]

Figure A.1-16 RSS Modeling Considered for Total Worth Bias Study

[[

]]

Figure A.2-1 Spectral Zones Flibe and TRISO Kernel Temperature Outputs from Input Sensitivity Analyses

[[

]]

Figure A.2-2 Axial Reflector Temperature Boundaries (top) and Maximum Axial Fluence Distribution (bottom)

[[

]]

APPENDIX B. Verification and Validation

B.1 Discrete Elements Modeling

[[

]]

B.2 Thermal-Hydraulics

[[

]]

B.2.1 Porous Media Closures Applicability

B.2.1.1 Pressure Drop

[[

]]

[[
]]

B.2.1.2 Pebble-Flibe Heat Transfer Coefficient

[[
]]

B.2.2.1 [[ ]]

B.2.2.1.1 Bed Heat Transfer

[[
]]

B.2.2.1.2 Reflector Heat Transfer

[[
]]

[[

]]

Table B.1-1 Pebble Bed Cylinder Configurations

[[

]]

Table B.2-1 [[ ]]

[[

]]

Table B.2-2 [[ ]]

[[

]]

Table B.2-3 Flow Rates and Pebble Powers for Pebble Bed Case Cylinder 2

[[

]]

Table B.2-4 [[ ]]

[[

]]

Table B.2-5 [[ ]]

[[

]]

Table B.2-6 [[ ]]

[[

]]

Figure B.1-1 Total number of pebbles inside the core vs DEM COF

[[

]]

Figure B.1-2 [[

]]

[[

]]

Figure B.2-1 Flibe and pebble surface temperature axial profiles [[ ]]

[[

]]

Figure B.2-2 Flibe and reflector surface temperatures axial for Re = 250 and reflector heating

[[

]]

APPENDIX C. Neutronics PIRT Results for the KP-FHR

[[

]]

[[

]]